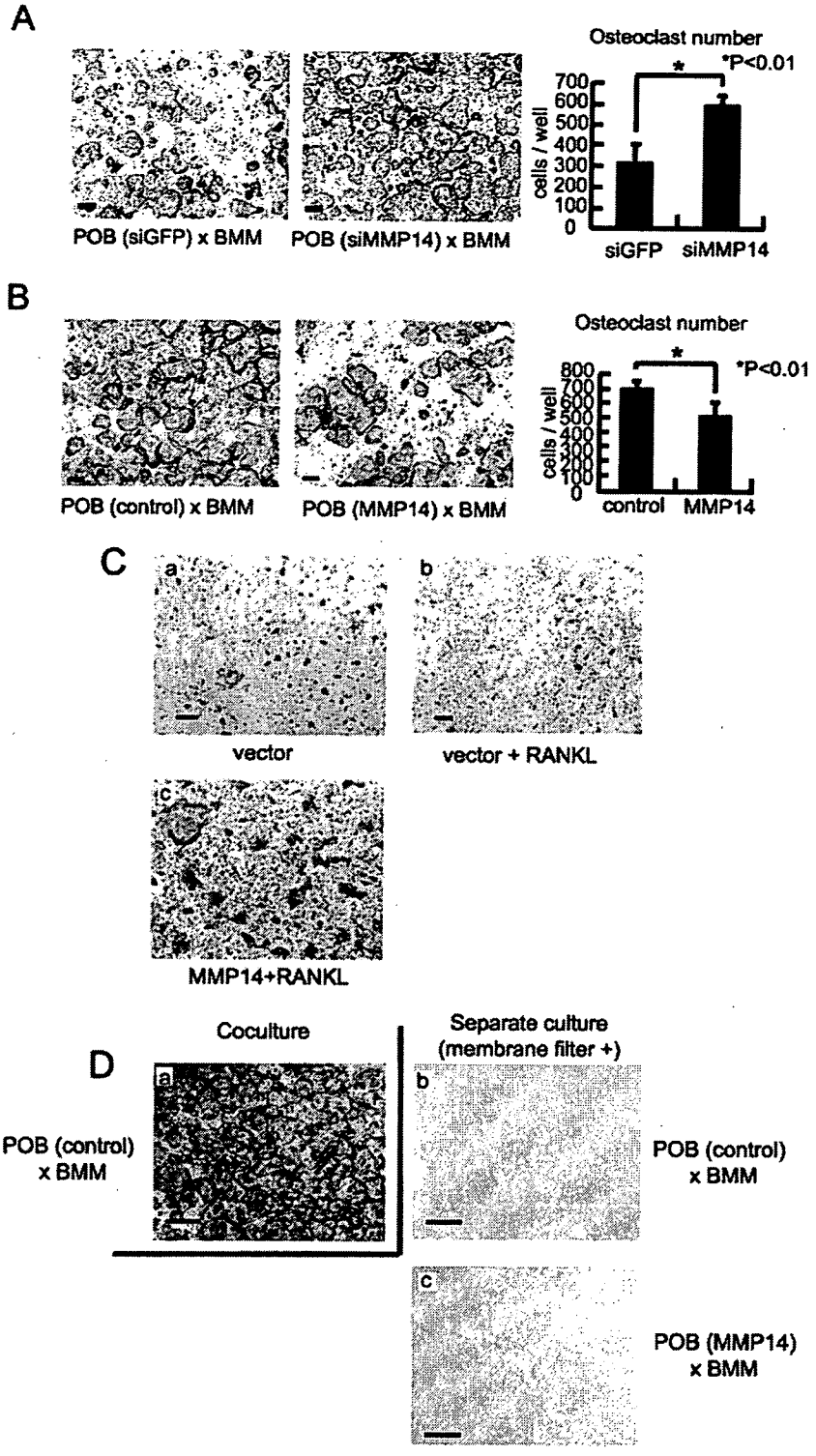

FIGURE 4. **MMP14 down-regulates osteoclastogenesis via RANKL cleavage.** *A* and *B*, coculture of primary osteoblasts infected with control siGFP or siMMP14 retrovirus (*A*), control or MMP14 retrovirus (*B*), and bone marrow macrophages. After 5 days' coculture, osteoclasts were stained with tartrate-resistant acid phosphatase and counted. *Right panel* shows the mean number of osteoclasts per well ($n = 4$). *, significantly different, $p < 0.01$. *C*, bone marrow macrophages were incubated with culture media of 293T cells transfected with pcDNA3.1-V5HisA (*a*), 1:1 mixture of pcDNA3.1-V5HisA and pcDNA3.1-RANKL-V5HisB (*b*), and 1:1 mixture of pcDNA3.1-RANKL-V5HisB and pcDNA3.1-MMP14-V5HisA (*c*), supplemented with M-CSF (10 ng/ml) for 4 days. *D*, bone marrow macrophages were cultured with primary osteoblasts infected with control (*a* and *b*) or MMP14 retrovirus (*c*) with (*b* and *c*; separate culture) or without (*a*; coculture) membrane filter between the two types of cells for 5 days. *Scale bars* = 200 μm (*A–C*) and 100 μm (*D*). *POB*, primary osteoblasts; *BMM*, bone marrow macrophages.

results indicated that ADAM10 and MMP14 are two major RANKL sheddases in TM8B2 cells.

MMP14 Cleaves RANKL in Primary Osteoblasts—We next examined the RANKL sheddases in primary osteoblasts. When primary osteoblasts were stimulated with $1\alpha,25(OH)_2D_3$, PGE_2, and IL-1, two bands appeared in the culture media with the same molecular masses (~22 and 21 kDa) as those observed in TM8B2 cells transfected with full-length RANKL without epitope tag (Fig. 3*A* and data not shown), but the lower band was more prominent. The expression of MMP14 was also much higher than that of MT2-, MT3-, or MT5-MMP in osteoblasts, suggesting that MMP14 is the major RANKL sheddase in primary osteoblasts (Fig. 2*D*). We constructed retrovirus vectors of siMMP14 that efficiently suppressed MMP14 expression in primary osteoblasts (Fig. 3*B*). When osteoblasts were infected with siMMP14 retrovirus, the lower band was diminished in the culture medium and membrane-bound RANKL was increased in the cell lysate (Fig. 3*A*). The concentration of soluble RANKL in the culture media and membrane-bound RANKL in the cell lysates was also measured by ELISA. A significant decrease in soluble RANKL and an increase in membrane-bound RANKL was observed by MMP14 knockdown (Fig. 3*C*), consistent with the results of Western blot analysis. Conversely, overexpression of MMP14 in primary osteoblasts increased the lower band of soluble RANKL in the culture media and reduced membrane-bound RANKL in the cell lysates (Fig. 3, *D* and *E*). To further confirm the role of MMP14 in RANKL shedding in osteoblasts, we analyzed primary osteoblasts obtained from MMP14 knock-out mice. When primary osteoblasts of MMP14-deficient mice were stimulated with $1\alpha,25(OH)_2D_3$, PGE_2, and IL-1, only the upper band of soluble RANKL was observed in the culture medium (Fig. 3*F*). The amount of soluble RANKL was markedly reduced in

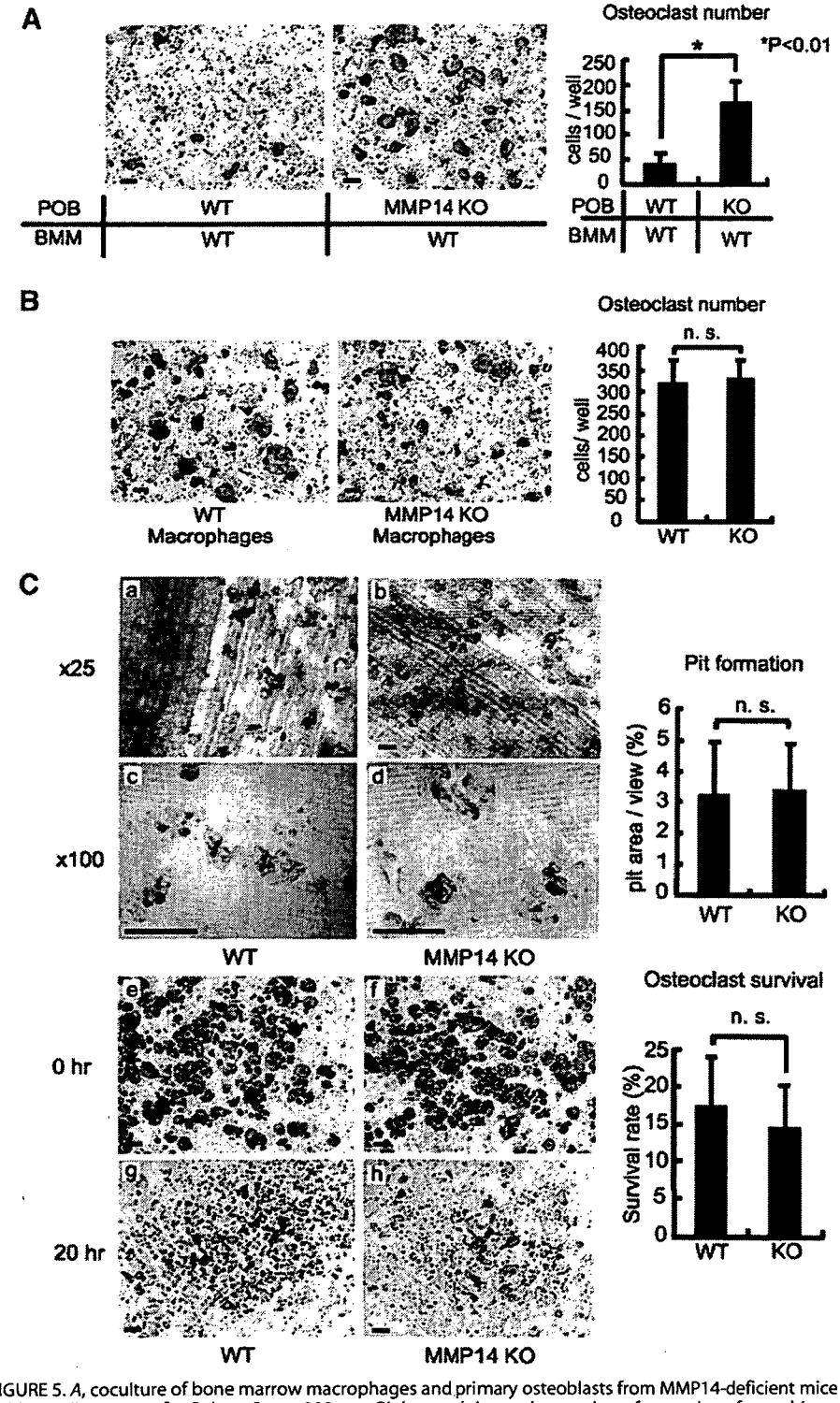

FIGURE 5. *A*, coculture of bone marrow macrophages and primary osteoblasts from MMP14-deficient mice or wild-type littermates for 5 days. *Bar* = 200 μm. *Right panel* shows the number of osteoclasts formed ($n = 4$). *, significantly different, $p < 0.01$. *POB*, primary osteoblasts; *BMM*, bone marrow macrophages. *B*, MMP14 deficiency does not affect osteoclast differentiation. Macrophages of MMP14 knock-out mice or wild-type littermates were cultured in the presence of M-CSF and RANKL for 6 days. *Scale bar* = 200 μm. *Right panel* shows the number of osteoclasts ($n = 4$). *n.s.*, not significantly different. *C*, MMP14 deficiency does not affect bone resorption activity or survival rate of osteoclasts. Macrophages of MMP14 knock-out mice (*b*, *d*, *f*, and *h*) or wild-type littermates (*a*, *c*, *e*, and *g*) were cocultured with wild-type primary osteoblasts on the collagen gel matrix for 7 days and subjected to the pit formation assay (*a–d*) and the survival assay (*e–h*). *Scale bar* = 200 μm. *Graphs* are the number of pit formation rate (*upper*), and osteoclast survival rate (*lower*) ($n = 4$). *n.s.*, not significantly different.

the medium, and membrane-bound RANKL was increased (Fig. 3*G*).

RANKL Shedding Negatively Regulates Osteoclastogenesis—To determine the role of MMP14 in the osteoclastogenic activity of osteoblasts, we cocultured osteoblasts infected with siMMP14 retrovirus with bone marrow macrophages. The siMMP14 retrovirus-infected osteoblasts, in which RANKL shedding activity was suppressed and membrane-bound RANKL was increased, stimulated osteoclastogenesis more effectively than control cells (Fig. 4*A*). Conversely, overexpression of MMP14 in primary osteoblasts suppressed osteoclastogenesis (Fig. 4*B*). These results suggest that membrane-bound RANKL induces osteoclastogenesis more efficiently than soluble RANKL, and the ectodomain shedding of RANKL by MMP14 negatively regulates osteoclastogenesis.

We then examined the osteoclastogenic activity of the soluble RANKL generated by MMP14. The culture media of 293T cells transfected with RANKL and MMP14 expression vectors were collected 48 h after transfection, and bone marrow macrophages were cultured in media supplemented with 10 ng/ml M-CSF (Fig. 4*C*). When macrophages were cultured in media recovered from the empty vector or RANKL expression vector-transfected cell cultures, mature osteoclasts did not form, even in the presence of M-CSF. In contrast, the culture media from the cells transfected with both RANKL and MMP14 expression vectors induced osteoclast formation, indicating that the soluble RANKL generated by MMP14 had osteoclastogenic activity. When primary osteoblasts overexpressing MMP14 by retrovirus vectors and bone marrow cells were cultured separately using cell culture inserts, which allow the passage of culture media but prevent cell-cell contact, and were stimulated with $1\alpha,25(OH)_2D_3$, PGE_2, and IL-1, very few osteoclasts were formed (Fig. 4*D*). These results suggest that the amount of endogenous

soluble RANKL generated in primary osteoblasts is not sufficient to induce osteoclastogenesis in our assay system.

We finally analyzed the osteoclastogenic activity of MMP14-deficient osteoblasts. When normal bone marrow macrophages were cocultured with osteoblasts from MMP14-deficient mice, osteoclasts were formed more efficiently than in cocultures with wild-type osteoblasts (Fig. 5*A*). On the other hand, bone marrow macrophages from MMP14-deficient mice differentiated into mature osteoclasts with the same efficiency as wild-type cells (Fig. 5*B*), and their bone-resorbing activity and survival rate were comparable (Fig. 5*C*). Consistent with these *in vitro* observations, soft x-ray images of MMP14-deficient mice displayed osteoporosis (Fig. 6*A*). Histologic sections showed thin cortical bone, decreased cancellous bone, and increased osteoclasts on the trabecular bone surface, which agreed with a previous report (33) (Fig. 6*B*). These data suggested that the increased osteoclast number in MMP14-deficient mice is due to the increase in membrane-bound RANKL in osteoblasts.

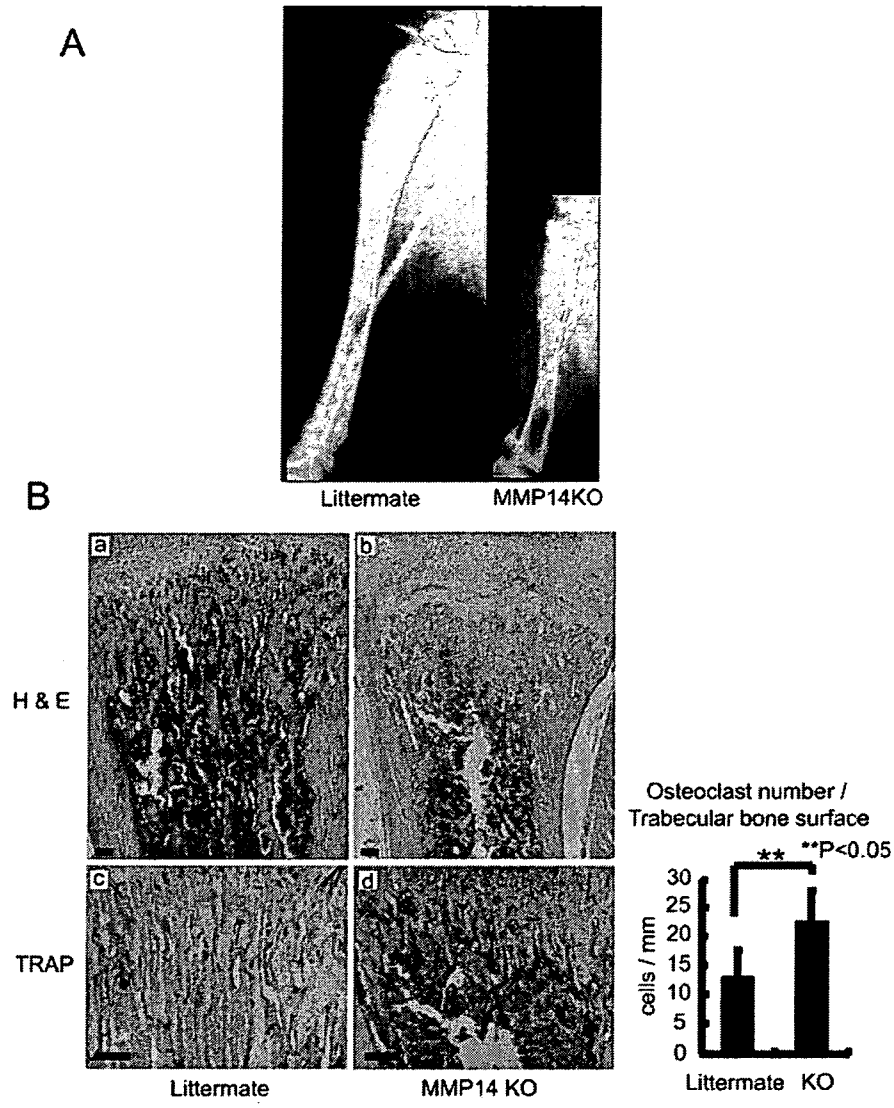

FIGURE 6. **Severe osteopenia and increased osteoclastogenesis in MMP14-deficient mice.** *A*, soft x-ray images of the left tibia of MMP14 knock-out mouse and the littermate. *B*, histologic analysis of proximal tibia of MMP14 knock-out mouse (*b* and *d*) or the wild-type littermate (*a* and *c*) stained with H&E (*a* and *b*) or tartrate-resistant acid phosphatase (*c* and *d*). *Scale bar* = 100 μm. *Right panel* shows the number of osteoclasts per trabecular bone surface ($n = 4$). **, significantly different, $p < 0.05$.

DISCUSSION

There is accumulating evidence that protein ectodomain shedding affects a large number of cellular membrane proteins, including TNF family members, but the functional outcome of shedding depends on the particular substrate protein. For example, TNF-α is cleaved by some proteinases such as TNF-α converting enzyme and released into the circulatory system to exhibit strong systemic effects (13, 14). In contrast, Fas ligand, which is a strong apoptosis inducer, has reduced effects in its soluble form (19). RANKL is a member of the TNF family of cytokines, and recent studies indicate that RANKL is essential in skeletal homeostasis for regulating the differentiation and activation of osteoclasts. Membrane-bound RANKL is proteolytically processed to generate the soluble form, but the specific proteinases involved in RANKL shedding and its physiologic and pathologic importance are not known. Western blot analysis revealed that there are two different cleaved products in the supernatants of both TM8B2 bone marrow stromal cells and primary osteoblasts, and the lower band was the major band in primary osteoblasts (Fig. 3*A*). The N-terminal sequence of the upper band coincides with the constitutive cleavage site previously reported in COS7 cells, and that of the lower band coincides with the putative MMP cleavage site. The lower band was decreased in the presence of an MMP inhibitor FR255031, and both bands were diminished by treatment with FR217840, which inhibits both MMPs and ADAMs. Previous studies also demonstrated that various MMPs and ADAMs have RANKL shedding activity (17, 20, 34–36). Therefore, we first analyzed the RANKL shedding activity of several MMPs and ADAMs using the previously reported RANKL shedding assay (20). MMP7, MMP19, ADAM9, ADAM10, ADAM17, ADAM19, MMP14, MT2, MT3, MT4, MT5, and MT6-MMP had tRANKL-SEAP shedding activity. Among these proteinases, ADAM9, ADAM10, ADAM19, MMP14, MT2, MT3, and MT5-MMP cleaved full-length RANKL. Although ADAM9 and ADAM19 had RANKL shedding activity, the molecular weights of the cleaved products were different from those con-

stitutively generated in TM8B2 cells and primary osteoblasts. Among MT-MMPs, MMP14 was predominantly expressed in TM8B2 and primary osteoblasts. MMP7 was reported to cleave RANKL *in vitro* or under overexpressing conditions and has an important role in prostate cancer-induced osteolysis (34). Although MMP7 had tRANKL-SEAP shedding activity, it did not cleave full-length RANKL in our assay system. Blobel and co-workers (17) demonstrated that ADAM17 (TNF-α converting enzyme) cleaves a partial fragment of RANKL protein, but not full-length RANKL (35), and we confirmed that ADAM17 did not cleave full-length RANKL. Although MMP13 deficiency leads to skeletal abnormalities (37), it did not cleave tRANKL-SEAP or full-length RANKL. These data, in combination with the results of siRNA experiments, led us to speculate that ADAM10 and MMP14 were major RANKL sheddases in TM8B2 cells and osteoblasts, although it is possible that other proteinases are involved in RANKL shedding in some pathologic conditions in which they are up-regulated. The functional difference between MMP14-cleaved RANKL and ADAM10-cleaved RANKL is currently under investigation.

In the culture media of primary osteoblasts, the lower molecular weight product was much more predominant than the higher molecular weight product, indicating that MMP14 is the major RANKL sheddase in primary osteoblasts. This was further confirmed by the results obtained from MMP14 knockdown osteoblasts and MMP14-deficient osteoblasts, in which the lower molecular weight band was almost completely diminished and the concentration of soluble RANKL was severely reduced.

Reduced MMP14 expression in primary osteoblasts by siRNA or its deficiency in MMP14 knock-out mouse osteoblasts reduced RANKL shedding and increased membrane-bound RANKL, which led to increased osteoclastogenic activity in the cells. Although soluble RANKL produced by MMP14 induced osteoclastogenesis from bone marrow macrophages, the culture medium of primary osteoblasts treated with $1\alpha,25(OH)_2D_3$ and PGE_2 did not induce osteoclastogenesis (38), even when MMP14 was overexpressed. This was probably due to an insufficient amount of soluble RANKL, because the concentration of the soluble RANKL in the culture media was <1 ng/ml (data not shown), and the amount of recombinant soluble RANKL necessary to induce osteoclastogenesis *in vitro* was >10 ng/ml. Still, it is possible that when the expression of RANKL is highly up-regulated, soluble RANKL has substantial effects on general bone metabolism. Gao *et al.* reported that parathyroid hormone(1–34) not only increases RANKL but also decreases MMP14 production in human osteoblasts, which might result in the efficient up-regulation of bone resorption by increasing membrane-bound RANKL in the cells (39).

In MMP14-deficient mice, generalized osteopenia was observed. Although this might be partially due to the reduced bone formation, as previously reported (33), the osteoclast number was much higher in these mice, possibly due to the increased membrane-bound RANKL in the osteoblasts. In fact, the serum level of soluble RANKL in MMP14 knock-out mice was undetectable, even when they were injected with $1\alpha,25(OH)_2D_3$ (data not shown). These phenotypes are not due to cell autonomous defects in osteoclast precursors, because there were no abnormalities in osteoclast differentiation from MMP14-deficient macrophages or bone-resorbing function of mature osteoclasts.

We were unable to determine the role of ADAM10 in *in vivo* RANKL shedding or skeletal homeostasis, because ADAM10-deficient animals die at E9.5 due to defects in heart and central nervous system development (40). Therefore, future studies using cell-specific knock-out of ADAM10 are required.

To conclude, we identified MMP14 as a major endogenous RANKL sheddase in primary osteoblasts. RANKL shedding negatively affects local osteoclastogenesis by reducing membrane-bound RANKL in the skeletal environment.

Acknowledgments—We thank R. Yamaguchi (Dept. of Orthopaedic Surgery, The University of Tokyo), who provided expert technical assistance. FR255031 and FR217840 were generously provided by Astellas Pharma Inc. (Tokyo, Japan).

REFERENCES

1. Anderson, D. M., Maraskovsky, E., Billingsley, W. L., Dougall, W. C., Tometsko, M. E., Roux, E. R., Teepe, M. C., DuBose, R. F., Cosman, D., and Galibert, L. (1997) *Nature* **390,** 175–179
2. Wong, B. R., Rho, J., Arron, J., Robinson, E., Orlinick, J., Chao, M., Kalachikov, S., Cayani, E., Bartlett, F. S., 3rd, Frankel, W. N., Lee, S. Y., and Choi, Y. (1997) *J. Biol. Chem.* **272,** 25190–25194
3. Yasuda, H., Shima, N., Nakagawa, N., Yamaguchi, K., Kinosaki, M., Mochizuki, S., Tomoyasu, A., Yano, K., Goto, M., Murakami, A., Tsuda, E., Morinaga, T., Higashio, K., Udagawa, N., Takahashi, N., and Suda, T. (1998) *Proc. Natl. Acad. Sci. U. S. A.* **95,** 3597–3602
4. Lacey, D. L., Timms, E., Tan, H. L., Kelley, M. J., Dunstan, C. R., Burgess, T., Elliott, R., Colombero, A., Elliott, G., Scully, S., Hsu, H., Sullivan, J., Hawkins, N., Davy, E., Capparelli, C., Eli, A., Qian, Y. X., Kaufman, S., Sarosi, I., Shalhoub, V., Senaldi, G., Guo, J., Delaney, J., and Boyle, W. J. (1998) *Cell* **93,** 165–176
5. Kong, Y. Y., Feige, U., Sarosi, I., Bolon, B., Tafuri, A., Morony, S., Capparelli, C., Li, J., Elliott, R., McCabe, S., Wong, T., Campagnuolo, G., Moran, E., Bogoch, E. R., Van, G., Nguyen, L. T., Ohashi, P. S., Lacey, D. L., Fish, E., Boyle, W. J., and Penninger, J. M. (1999) *Nature* **402,** 304–309
6. Tanaka, S., Nakamura, K., Takahasi, N., and Suda, T. (2005) *Immunol. Rev.* **208,** 30–49
7. Wong, B. R., Josien, R., Lee, S. Y., Vologodskaia, M., Steinman, R. M., and Choi, Y. (1998) *J. Biol. Chem.* **273,** 28355–28359
8. Takayanagi, H., Kim, S., Koga, T., Nishina, H., Isshiki, M., Yoshida, H., Saiura, A., Isobe, M., Yokochi, T., Inoue, J., Wagner, E. F., Mak, T. W., Kodama, T., and Taniguchi, T. (2002) *Dev. Cell* **3,** 889–901
9. Tanaka, S., Nakamura, I., Inoue, J., Oda, H., and Nakamura, K. (2003) *J. Bone Miner. Metab.* **21,** 123–133
10. Kong, Y. Y., Yoshida, H., Sarosi, I., Tan, H. L., Timms, E., Capparelli, C., Morony, S., Oliveira-dos-Santos, A. J., Van, G., Itie, A., Khoo, W., Wakeham, A., Dunstan, C. R., Lacey, D. L., Mak, T. W., Boyle, W. J., and Penninger, J. M. (1999) *Nature* **397,** 315–323
11. Dougall, W. C., Glaccum, M., Charrier, K., Rohrbach, K., Brasel, K., De Smedt, T., Daro, E., Smith, J., Tometsko, M. E., Maliszewski, C. R., Armstrong, A., Shen, V., Bain, S., Cosman, D., Anderson, D., Morrissey, P. J., Peschon, J. J., and Schuh, J. (1999) *Genes Dev.* **13,** 2412–2424
12. Bucay, N., Sarosi, I., Dunstan, C. R., Morony, S., Tarpley, J., Capparelli, C., Scully, S., Tan, H. L., Xu, W., Lacey, D. L., Boyle, W. J., and Simonet, W. S. (1998) *Genes Dev.* **12,** 1260–1268
13. Kriegler, M., Perez, C., DeFay, K., Albert, I., and Lu, S. D. (1988) *Cell* **53,** 45–53
14. Black, R. A., Rauch, C. T., Kozlosky, C. J., Peschon, J. J., Slack, J. L., Wolfson, M. F., Castner, B. J., Stocking, K. L., Reddy, P., Srinivasan, S., Nelson, N., Boiani, N., Schooley, K. A., Gerhart, M., Davis, R., Fitzner, J. N., Johnson, R. S., Paxton, R. J., March, C. J., and Cerretti, D. P. (1997) *Nature* **385,**

729–733
15. Harris, R. C., Chung, E., and Coffey, R. J. (2003) *Exp. Cell Res.* **284,** 2–13
16. Prenzel, N., Zwick, E., Daub, H., Leserer, M., Abraham, R., Wallasch, C., and Ullrich, A. (1999) *Nature* **402,** 884–888
17. Lum, L., Wong, B. R., Josien, R., Becherer, J. D., Erdjument-Bromage, H., Schlondorff, J., Tempst, P., Choi, Y., and Blobel, C. P. (1999) *J. Biol. Chem.* **274,** 13613–13618
18. Nakashima, T., Kobayashi, Y., Yamasaki, S., Kawakami, A., Eguchi, K., Sasaki, H., and Sakai, H. (2000) *Biochem. Biophys. Res. Commun.* **275,** 768–775
19. Schneider, P., Holler, N., Bodmer, J. L., Hahne, M., Frei, K., Fontana, A., and Tschopp, J. (1998) *J. Exp. Med.* **187,** 1205–1213
20. Hikita, A., Kadono, Y., Chikuda, H., Fukuda, A., Wakeyama, H., Yasuda, H., Nakamura, K., Oda, H., Miyazaki, T., and Tanaka, S. (2005) *J. Biol. Chem.* **280,** 41700–41706
21. Sato, H., Takino, T., Okada, Y., Cao, J., Shinagawa, A., Yamamoto, E., and Seiki, M. (1994) *Nature* **370,** 61–65
22. Takino, T., Sato, H., Shinagawa, A., and Seiki, M. (1995) *J. Biol. Chem.* **270,** 23013–23020
23. Tanaka, M., Sato, H., Takino, T., Iwata, K., Inoue, M., and Seiki, M. (1997) *FEBS Lett.* **402,** 219–222
24. Itoh, Y., Kajita, M., Kinoh, H., Mori, H., Okada, A., and Seiki, M. (1999) *J. Biol. Chem.* **274,** 34260–34266
25. Kojima, S., Itoh, Y., Matsumoto, S., Masuho, Y., and Seiki, M. (2000) *FEBS Lett.* **480,** 142–146
26. Miyamori, H., Takino, T., Kobayashi, Y., Tokai, H., Itoh, Y., Seiki, M., and Sato, H. (2001) *J. Biol. Chem.* **276,** 28204–28211
27. Suda, T., Jimi, E., Nakamura, I., and Takahashi, N. (1997) *Methods Enzymol.* **282,** 223–235
28. Yamamoto, A., Miyazaki, T., Kadono, Y., Takayanagi, H., Miura, T., Nishina, H., Katada, T., Wakabayashi, K., Oda, H., Nakamura, K., and Tanaka, S. (2002) *J. Bone Miner. Res.* **17,** 612–621
29. Kitamura, T. (1998) *Int. J. Hematol.* **67,** 351–359
30. Ohtake, Y., Tojo, H., and Seiki, M. (2006) *J. Cell Sci.* **119,** 3822–3832
31. Ishikawa, T., Nishigaki, F., Miyata, S., Hirayama, Y., Minoura, K., Imanishi, J., Neya, M., Mizutani, T., Imamura, Y., Naritomi, Y., Murai, H., Ohkubo, Y., Kagayama, A., and Mutoh, S. (2005) *Br. J. Pharmacol.* **144,** 133–143
32. Ishikawa, T., Nishigaki, F., Miyata, S., Hirayama, Y., Minoura, K., Imanishi, J., Neya, M., Mizutani, T., Imamura, Y., Ohkubo, Y., and Mutoh, S. (2005) *Eur. J. Pharmacol.* **508,** 239–247
33. Holmbeck, K., Bianco, P., Caterina, J., Yamada, S., Kromer, M., Kuznetsov, S. A., Mankani, M., Robey, P. G., Poole, A. R., Pidoux, I., Ward, J. M., and Birkedal-Hansen, H. (1999) *Cell* **99,** 81–92
34. Lynch, C. C., Hikosaka, A., Acuff, H. B., Martin, M. D., Kawai, N., Singh, R. K., Vargo-Gogola, T. C., Begtrup, J. L., Peterson, T. E., Fingleton, B., Shirai, T., Matrisian, L. M., and Futakuchi, M. (2005) *Cancer Cell* **7,** 485–496
35. Schlondorff, J., Lum, L., and Blobel, C. P. (2001) *J. Biol. Chem.* **276,** 14665–14674
36. Chesneau, V., Becherer, J. D., Zheng, Y., Erdjument-Bromage, H., Tempst, P., and Blobel, C. P. (2003) *J. Biol. Chem.* **278,** 22331–22340
37. Inada, M., Wang, Y., Byrne, M. H., Rahman, M. U., Miyaura, C., Lopez-Otin, C., and Krane, S. M. (2004) *Proc. Natl. Acad. Sci. U. S. A.* **101,** 17192–17197
38. Takahashi, N., Akatsu, T., Udagawa, N., Sasaki, T., Yamaguchi, A., Moseley, J. M., Martin, T. J., and Suda, T. (1988) *Endocrinology* **123,** 2600–2602
39. Guo, L. J., Xie, H., Zhou, H. D., Luo, X. H., Peng, Y. Q., and Liao, E. Y. (2004) *Endocr. Res.* **30,** 369–377
40. Hartmann, D., de Strooper, B., Serneels, L., Craessaerts, K., Herreman, A., Annaert, W., Umans, L., Lubke, T., Lena Illert, A., von Figura, K., and Saftig, P. (2002) *Hum. Mol. Genet.* **11,** 2615–2624

Th17 functions as an osteoclastogenic helper T cell subset that links T cell activation and bone destruction

Kojiro Sato,[1,3] Ayako Suematsu,[1,3] Kazuo Okamoto,[1,3] Akira Yamaguchi,[2] Yasuyuki Morishita,[4] Yuho Kadono,[5] Sakae Tanaka,[5] Tatsuhiko Kodama,[6] Shizuo Akira,[7] Yoichiro Iwakura,[8] Daniel J. Cua,[9] and Hiroshi Takayanagi[1,3,10]

[1]Department of Cell Signaling, [2]Department of Oral Pathology, Graduate School, and [3]COE Program for Frontier Research on Molecular Destruction and Reconstruction of Tooth and Bone, Tokyo Medical and Dental University, Tokyo 113-8549, Japan
[4]Department of Human Pathology and [5]Department of Orthopaedic Surgery, Graduate School of Medicine, University of Tokyo, Tokyo 113-0033, Japan
[6]Department of Systems Biology and Medicine, Research Center for Advanced Science and Technology, University of Tokyo, Tokyo 153-8904, Japan
[7]Department of Host Defence, Research Institute for Microbial Diseases, Osaka University, Osaka 565-0871, Japan
[8]Center for Experimental Medicine, Institute of Medical Science, University of Tokyo, Tokyo 108-8639, Japan
[9]Discovery Research, DNAX Research Inc., Palo Alto, CA 94304
[10]Solution Oriented Research for Science and Technology (SORST), Japan Science and Technology Agency (JST), Saitama 332-0012, Japan

In autoimmune arthritis, traditionally classified as a T helper (Th) type 1 disease, the activation of T cells results in bone destruction mediated by osteoclasts, but how T cells enhance osteoclastogenesis despite the anti-osteoclastogenic effect of interferon (IFN)-γ remains to be elucidated. Here, we examine the effect of various Th cell subsets on osteoclastogenesis and identify Th17, a specialized inflammatory subset, as an osteoclastogenic Th cell subset that links T cell activation and bone resorption. The interleukin (IL)-23–IL-17 axis, rather than the IL-12–IFN-γ axis, is critical not only for the onset phase, but also for the bone destruction phase of autoimmune arthritis. Thus, Th17 is a powerful therapeutic target for the bone destruction associated with T cell activation.

CORRESPONDENCE
Hiroshi Takayanagi:
taka.csi@tmd.ac.jp

Abbreviations used: BMC, BM cell; BMM, BM-derived monocyte/macrophage precursor cell; M-CSF, macrophage colony-stimulating factor; MNC; multinucleated cell; PGE_2, prostaglandin E_2; RA, rheumatoid arthritis; RANKL, receptor activator of NF-κB ligand; TRAP, tartrate-resistant acid phosphatase; T reg, regulatory T; $VitD_3$, 1,25 $(OH)_2$ vitamin D_3.

Skeletal homeostasis is dynamically influenced by the immune system (1–3), and lymphocyte- or macrophage-derived cytokines are among the most potent mediators of osteoimmunological regulation (3–7). Therefore, the effect of individual cytokines on bone cells has been extensively studied (3–7), but the subset of immune cells with selective cytokine production that specifically affects bone cell differentiation has not been well characterized. Upon activation, $CD4^+$ T cells undergo distinct developmental pathways to the specialized effector subsets: Th1 cells produce IFN-γ and regulate cellular immunity, whereas Th2 cells produce IL-4 and IL-5 and mediate humoral immunity (8). In addition, accumulating evidence suggests that newly recognized IL-17–producing T (Th17) cells have a crucial role in autoimmune inflammation (9, 10). $CD4^+CD25^+Foxp3^+$ regulatory T (T reg) cells also constitute a distinct subset that prevents immune pathology through suppression of pathogenic T cells (11). Activation of $CD4^+$ T cells is often linked to pathological bone resorption (3, 4), but the distinct $CD4^+$ T cell subset that induces the differentiation of bone-resorbing osteoclasts has not been identified (2, 3).

Osteoclasts are multinucleated cells (MNCs) of monocyte/macrophage lineage that degrade bone matrix and dynamically remodel the skeleton (4–6). The generation of osteoclasts is physiologically supported by mesenchymal cells such as osteoblasts, which provide essential signals for differentiation of the osteoclast lineage: macrophage colony-stimulating factor (M-CSF), receptor activator of NF-κB ligand (RANKL), and costimulatory signals for RANKL (12). RANKL is the key osteoclastogenic cytokine expressed by osteoclastogenesis-supporting mesenchymal cells, but the same molecule has

The online version of this article contains supplemental material.

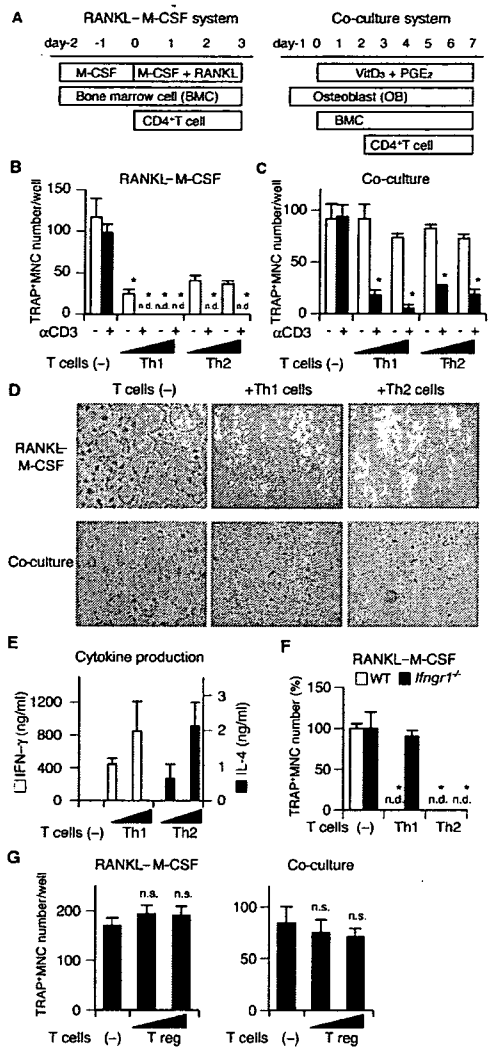

Figure 1. Effects of Th1, Th2, and T reg cells on in vitro osteoclastogenesis. (A) Schematics of two culture systems for osteoclast differentiation and Th cell addition. In the RANKL-M-CSF system, mouse nonadherent BMCs were stimulated with M-CSF for 2 d and adherent cells were used as BMMs. After BMMs were stimulated with recombinant RANKL and M-CSF for 3 d, the formation of $TRAP^+$ MNCs was analyzed. In the co-culture system, BMCs were co-cultured with osteoblasts stimulated with $VitD_3$ and PGE_2, and the formation of $TRAP^+$ MNCs was observed 7 d after the addition of BMCs. (B) Inhibitory effects of Th1 and Th2 cells on $TRAP^+$ MNC formation in the RANKL-M-CSF system. Th cells (4,000 or 20,000 cells/ml) were added at the same time as RANKL (day 0) with (black bars) or without (white bars) anti-CD3 mAb. n.d., not detected. (C) Inhibitory effects of Th1 and Th2 cells on $TRAP^+$ MNC formation in the co-culture system. The same number of T cells as in B was added 2 d after BMC addition (day 2). (D) Microphotographs of the in vitro osteoclast formation systems in the presence of Th1 or Th2 cells (20,000 cells/ml) with anti-CD3 mAb (TRAP staining). (E) Cytokine profile of culture supernatants in the presence of Th cells and 1 μg/ml of soluble anti-CD3 mAb (the RANKL-M-CSF system on day 2). Without restimulation by anti-CD3 mAb, cytokine production was much less than this result and was difficult to detect after 2-d culture with osteoclast precursor cells (not depicted). (F) Effects of Th1 and Th2 cells (20,000 cells/ml plus anti-CD3 mAb) on WT or IFN-γ receptor-deficient ($Ifngr1^{-/-}$) osteoclast precursor cells. (G) Effects of isolated $CD4^+CD25^+$ T reg cells (4,000 or 20,000 cells/ml plus anti-CD3 mAb) on osteoclastogenesis in vitro. n.s., not significantly different. The survival of a considerable number of T reg cells after 3 d was confirmed by CFSE staining (not depicted).

been shown to be expressed by T cells, indicating that RANKL is a molecule that bridges the skeletal and immune systems (4).

In autoimmune arthritis, bone destruction is attributable to excessive bone resorption by osteoclasts, the formation of which is directly and indirectly regulated by $CD4^+$ T cells infiltrating into the lesion (2, 3, 13, 14). Indirect effects are mainly mediated by inflammatory cytokines produced by macrophage-like synovial cells such as TNF-α and IL-1 that induce RANKL on synovial fibroblasts (14–16), but it is poorly understood how T cells exert direct effects (3). Although T cells express RANKL, the T cell–mediated positive effect is not easily observed because T cells also produce IFN-γ, which counterbalances the effect of the RANKL, making the net effect on osteoclastogenesis inhibitory (3, 13, 14). Although autoimmune arthritis has traditionally been assumed to be a Th1 disease (17, 18), there is controversy over the role of Th1 cells in the onset phase of the disease based on the observations that typical Th1 cytokines, such as IFN-γ, are not always highly expressed in the lesion (19, 20), and that collagen-induced arthritis is exacerbated in mice lacking IFN-γ signaling (21, 22). Therefore, neither bone destruction nor inflammation may be attributable to Th1 cells. It is a critically important issue to determine the type of T cells linked to the activated osteoclastogenesis under such inflammatory conditions.

Recently, it has been reported that the IL-23–IL-17 axis, rather than the IL-12–IFN-γ axis, is critical for the onset of autoimmune arthritis (23, 24). It is also reported that IL-17 is detectable in the synovial fluid from rheumatoid arthritis (RA) patients and enhances osteoclastogenesis by inducing RANKL on mesenchymal cells (25). Here, we explored the effects of various $CD4^+$ T cell subsets on osteoclast differentiation and identified Th17 cells as the exclusive osteoclastogenic T cell subset among the known $CD4^+$ T cell lineages. The importance of the IL-23–IL-17 axis in the bone destruction phase was underscored by the observations in mice lacking either IL-17 or IL-23 (p19). We also found that the mRNA expression of *RANKL* correlates with that of *IL-23* (*IL23A*), but not that of *IL-12* (*IL12A*), in the synovial tissues of RA patients. Collectively, these results suggest that autoimmune arthritis can be deemed a Th17-type disease in terms of both the onset and destruction phases and provide a molecular basis for targeting the IL-23–IL-17 axis in the treatment of RA.

RESULTS

Effects of Th1, Th2, and T reg cells on osteoclastogenesis

Although the effects of activated T cells on osteoclastogenesis have been documented in previous reports (13, 14, 26), these

T cells were only stimulated by anti-CD3 antibody or PMA and the characterization of the T cells was not strictly performed. In this study, to investigate the effects of effector Th cell subsets on osteoclastogenesis, we added Th subsets, which were strictly developed under Th1 or Th2 conditions. Purified $CD4^+$ T cells were stimulated with anti-CD3/CD28 mAbs in the presence of either IL-12 (with anti–IL-4 mAb) or IL-4 (with anti–IFN-γ mAb) for Th1 or Th2 polarization. The Th cells were added to the two types of in vitro osteoclast differentiation systems: osteoclast precursor cells derived from BM cells (BMCs) were stimulated with recombinant RANKL and M-CSF (the RANKL–M-CSF system), or co-cultured with osteoblasts in the presence of 1,25 $(OH)_2$ vitamin D_3 ($VitD_3$) and prostaglandin E_2 (PGE_2) (the co-culture system), and the formation of MNCs stained for tartrate-resistant acid phosphatase (TRAP), a marker enzyme for osteoclasts, was evaluated (Fig. 1 A). When Th1 or Th2 cells were added to the RANKL–M-CSF system at the same time as RANKL, both subsets had a marked inhibitory effect on the formation of $TRAP^+$ MNCs and the inhibitory effects were dependent on the number of added T cells (Fig. 1, B and D). These inhibitory effects were significantly enhanced by re-stimulation with soluble anti-CD3 mAb, suggesting that re-stimulation of T cell receptor augments the polarized cytokine secretion and the inhibitory effects on osteoclastogenesis. If Th1 or Th2 cells were added to the co-culture system 2 d after BMC addition, the inhibitory effects of both subsets on osteoclastogenesis were exerted only by T cells restimulated with anti-CD3 mAb (Fig. 1, C and D). Th1 and Th2 cells both had less suppressive effects in the co-culture system, possibly because osteoblasts provide protection against the inhibitory effects through costimulatory signals (27) (see Discussion). As expected, the Th1 and Th2 subsets used in these experiments produced a significant amount of IFN-γ and IL-4, respectively (Fig. 1 E). The inhibitory effects of Th1 cells on osteoclastogenesis were completely abrogated on the BM-derived monocyte/macrophage precursor cells (BMMs) derived from IFN-γ receptor–deficient (*Ifngr1*$^{-/-}$) mice (28), indicating that IFN-γ is responsible for the Th1 cell–mediated inhibition of osteoclastogenesis (Fig. 1 F). We further analyzed the effects of $CD4^+CD25^+$ T reg cells on osteoclastogenesis in both systems, but they were found to have neither an enhancing nor an inhibitory effect (Fig. 1 G), suggesting that T reg cells are not directly related to the T cell–mediated regulation of bone resorption.

Characterization of MNCs induced by Th2 cells and IL-4

It has been reported that the inhibitory effect of IFN-γ on osteoclastogenesis is reduced if the osteoclast precursor cells encounter RANKL before IFN-γ stimulation, suggesting that RANKL-prestimulated preosteoclasts are resistant to such inhibitory cytokines (29). To test whether the inhibitory effects of Th cells on osteoclastogenesis are also dependent on the differentiation stage of the osteoclast precursor cells, we added the Th cells to the osteoclast formation systems 1 d later than in the previous experiment. Interestingly, the inhibitory effects of Th cells were less (Fig. 2 A). Although Th1 cells inhibited the formation of $TRAP^+$ MNCs under this condition, Th2 cells induced a normal number of $TRAP^+$ MNCs in the RANKL–M-CSF system and even an increased number in the co-culture system (Fig. 2 A).

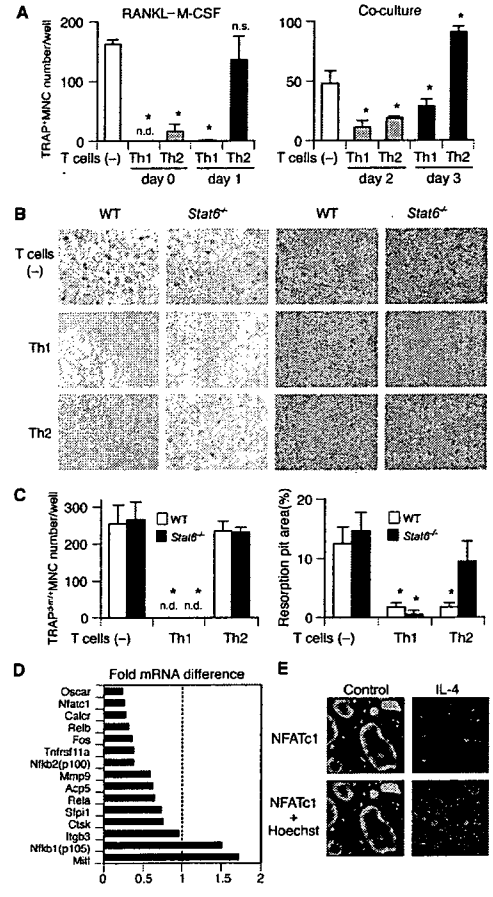

Figure 2. Formation of multinuclear cells with no bone-resorbing activity induced by Th2 cells and IL-4. (A) Inhibitory effects of Th1 and Th2 cells on osteoclastogenesis are reduced when T cells are added 1 d later. Th cells (20,000 cells/ml plus anti-CD3 mAb) were added on days 0 (at the same time as RANKL, gray bars) or 1 (black bars) to the RANKL–M-CSF system and on days 2 (2 d after BMC addition, gray bars) or 3 (black bars) to the co-culture system. (B) Microphotographs and (C) quantification of in vitro osteoclast formation (left, TRAP staining) and resorption pit formation (right). Th1 and Th2 cells (20,000 cells/ml plus anti-CD3 mAb) were added to WT or *Stat6*$^{-/-}$ osteoclast precursor cells on day 1. (D) Effect of IL-4 on mRNA expression of osteoclast-related genes in osteoclast precursor cells (GeneChip analysis). Osteoclast precursor cells were stimulated by 10 ng/ml IL-4 from day 1 in the RANKL–M-CSF system and harvested on day 3. Fold mRNA difference was calculated by dividing the average difference of the IL-4–treated sample by that of the control sample. The expressions of most of the osteoclast-specific genes are down-regulated. (E) Reduced expression of NFATc1 protein in the cells treated with IL-4. Osteoclast precursor cells were stimulated by 10 ng/ml IL-4 from day 1 in the RANKL–M-CSF system, fixed on day 3, and stained with anti-NFATc1 antibody followed by Alexa Fluoro 488–labeled secondary antibody.

These results appeared to suggest that Th2 cells increase osteoclastogenesis under certain conditions, but the MNCs induced in the presence of Th2 cells were only weakly stained for TRAP ($TRAP^{dim}$) and were incapable of bone resorption (Fig. 2, B and C). Even in the presence of Th2 cells, $TRAP^+$ MNCs with bone-resorbing activity were formed from BMMs derived from mice deficient in Stat6, which is an essential mediator of IL-4 signaling (30), suggesting that IL-4 is involved in the formation of $TRAP^{dim}$ MNCs. Consistent with this, the addition of IL-4 to the RANKL–M-CSF system at the same time as RANKL strongly inhibited $TRAP^+$ MNC formation, and the addition of IL-4 1 d later induced $TRAP^{dim}$ MNCs (Fig. S1, available at http://www.jem.org/cgi/content/full/jem.20061775/DC1). The effects of IL-4 were abrogated if added to Stat6-deficient cells, which generated $TRAP^+$ MNCs that were able to resorb bone.

To further characterize the $TRAP^{dim}$ MNCs induced by Th2 cells through IL-4, we performed a genome-wide microarray screening of the genes expressed in the $TRAP^{dim}$ MNCs (31). $TRAP^{dim}$ MNCs induced by IL-4 expressed a high level of genes characteristic of activated macrophages, including chemokine ligands and enzymes involved in allergic responses (Fig. S2, available at http://www.jem.org/cgi/content/full/jem.20061775/DC1). The expression of most of the genes important for osteoclast differentiation or functions was decreased (Fig. 2 D). The expression of NFATc1, an essential transcription factor for osteoclastogenesis (31, 32), was also revealed to be down-regulated by immunostaining (Fig. 2 E). Thus, the $TRAP^{dim}$ MNCs induced by Th2 cells are not authentic osteoclasts but rather should be classified as macrophage polykarions.

Th17 cells stimulate osteoclastogenesis through osteoclastogenesis-supporting cells

Because the above results show that neither Th1, Th2, nor T reg cells enhance osteoclastogenesis, we next focused on a newly identified $CD4^+$ T cell subset producing IL-17 called Th17 (33, 34). We suspected the Th17 subset to be a good candidate for the osteoclastogenic Th subset because it has been reported that IL-17 induces RANKL on mesenchymal cells and promotes osteoclastogenesis in vitro (25). Moreover, Th17 cells, which produce IL-17 (IL-17A) and its related cytokines such as IL-17F, but not IFN-γ or IL-4, are responsible for a variety of autoimmune inflammatory effects (9, 10). Recent studies suggest that TGF-β and IL-6 are essential for the initiation of Th17 differentiation and IL-23 is critical for expanding the population (35, 36). IL-23 is one of the IL-12 family cytokines and is a heterodimer consisting of the subunits p40 and p19 (9, 10). Even though IL-23 shares a p40 subunit and one of its receptor subunits (IL-12β1) with

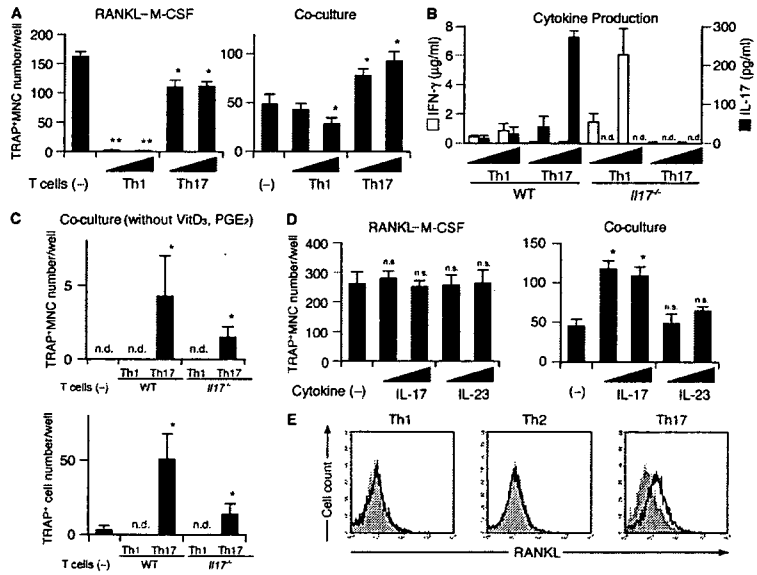

Figure 3. Enhanced osteoclastogenesis by Th17 cells in the co-culture system but not in the RANKL–M-CSF system. (A) Effects of Th1 and Th17 cells on the osteoclast differentiation systems. T cells (4,000 or 20,000 cells/ml plus anti-CD3 mAb) were added on day 1 to the RANKL–M-CSF system and on day 3 to the co-culture system. When the Th17 cells were added 1 d earlier, or in the absence of soluble anti-CD3 mAb, enhancement of osteoclastogenesis was not observed even in the co-culture system (not depicted). (B) Cytokine profile of the culture supernatants obtained on day 3 from the RANKL–M-CSF system in the presence of Th1 and Th17 cells derived from either WT or *Il17*$^{-/-}$ mice under the conditions described in A. (C) Effects of Th1 and Th17 cells derived from either WT or *Il17*$^{-/-}$ mice on the formation of $TRAP^+$ MNCs or $TRAP^+$ cells in the co-culture system in the absence of $VitD_3$ and PGE_2. T cells (20,000 cells/ml plus anti-CD3 mAb) were added on day 3. (D) Effects of recombinant IL-17 and IL-23 (2 or 10 ng/ml) on osteoclastogenesis in vitro. (E) Expression of RANKL on Th subsets. $CD4^+$ T cells cultured in each of the Th conditions for 3 d were restimulated with 1 μg/ml of plate-bound anti-CD3 mAb for 4 h and subjected to flow cytometric analysis using anti-RANKL mAb. Without the restimulation by anti-CD3 mAb, RANKL expression was barely detectable (not depicted).

IL-12, IL-23 and IL-12 selectively play critical roles in the regulation of Th1 and Th17 polarization, respectively.

To obtain the Th17 cells, we stimulated $CD4^+$ T cells with anti-CD3/CD28 mAbs in the presence of IL-23, anti–IFN-γ mAb, and anti–IL-4 mAb. In the presence of Th17 cells, $TRAP^+$ MNCs were efficiently formed in the RANKL–M-CSF system (Fig. 3 A) and possessed bone-resorbing activity (not depicted), although the efficiency is a little less than in the control culture without the T cells. Moreover, in the co-culture system, the Th17 cells significantly enhanced the formation of $TRAP^+$ MNCs (Fig. 3 A). Consistent with the previous reports, Th17 cells used in the above experiments produced a large amount of IL-17 but little IFN-γ, but Th1 cells did the opposite (Fig. 3 B). When Th17 cells were added to the co-culture system even in the absence of $VitD_3$ and PGE_2, the formation of $TRAP^+$ MNCs was observed (Fig. 3 C). The osteoclastogenic effects of Th17 cells in the co-culture system was greatly reduced when we used Th17 cells derived from *Il17*$^{-/-}$ mice (37), indicating that the IL-17 produced from Th17 cells is mainly responsible for the osteoclastogenic effects of Th17 cells. IL-23 or IL-17 had no effect on osteoclastogenesis in the RANKL–M-CSF system, but IL-17 promoted osteoclastogenesis in the co-culture system, suggesting that IL-17 does not directly act on osteoclast precursor cells but rather on osteoclastogenesis-supporting cells (Fig. 3 D). This is consistent with the previous report that IL-17 promotes osteoclastogenesis through the induction of RANKL on osteoblastic cells (25). These results show that Th17 is the only osteoclastogenic Th subset according to the currently accepted categorization of $CD4^+$ T cells, and that Th17 cells facilitate osteoclastogenesis, possibly through IL-17–mediated induction of RANKL on osteoblastic cells.

We evaluated the expression level of RANKL on the surface of Th cells and found that Th17 cells express a significant amount of RANKL, but Th1 cells express only a minimal amount (Fig. 3 E). Neither subset, however, exhibited promotive effects on osteoclastogenesis in the RANKL–M-CSF system (Fig. 3 A) or induced any $TRAP^+$ cells when added to the BMM culture in the absence of exogenous soluble RANKL (not depicted). Thus, it is evident that the RANKL expressed by Th cells alone is not sufficient to activate osteoclastogenesis (see Discussion).

The IL-23–IL-17 axis plays a critical role in inflammation-induced bone destruction in vivo

To clarify the role IL-17 and IL-23 play in bone metabolism in vivo, we investigated the phenotype of *Il17*$^{-/-}$ and *Il23a*$^{-/-}$ (lacking p19) (38) mice. There was no significant difference in bone mineral density as evaluated by dual-energy x-ray absorptiometry (Fig. 4 A). Microradiography also

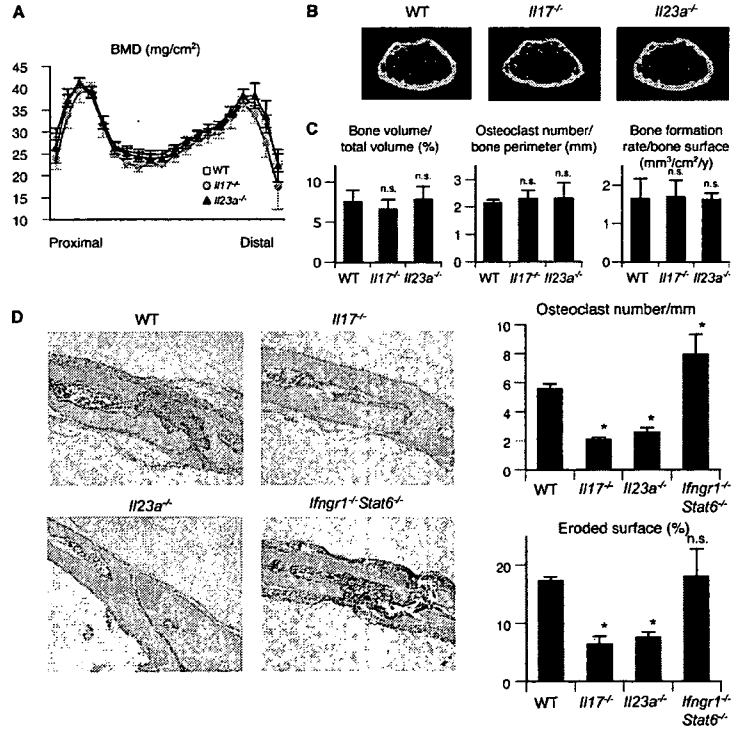

Figure 4. Contribution of IL-17 and IL-23 to the physiological and pathological bone resorption. (A) Bone mineral densities (measured in 20 longitudinal divisions of the femurs), (B) micro-computed tomography (at 10% length above the distal epiphyseal plate), and (C) bone morphometic analyses of WT, *Il17*$^{-/-}$, and *Il23a*$^{-/-}$ mice at the age of 12 wk. (D) Histological examination of calvarial bones of WT, *Il17*$^{-/-}$, and *Il23a*$^{-/-}$ mice treated with LPS (hematoxylin and TRAP staining). The degree of bone destruction was analyzed by the number of osteoclasts and the area of the eroded surface (%).

revealed no obvious abnormality in skeletal development (Fig. 4 B). Bone morphometric analyses revealed the parameters of bone resorption and formation to be normal even in the mutant mice (Fig. 4 C), indicating that neither IL-17 nor IL-23 is involved in the physiological regulation of bone homeostasis.

To further investigate the role of IL-17 and IL-23 in the disease conditions characterized by enhanced osteoclastogenesis associated with T cell activation, we used an LPS-induced model of inflammatory bone destruction, which is not induced by an autoantigen but is T cell dependent (14, 39). Because it is well documented that IL-17 and IL-23 play an important role in the development of autoimmune arthritis (23, 24), we used this inflammatory bone destruction model to evaluate their role in the osteoclast-mediated destruction phase. LPS injection into the calvarial bone results in severe bone destruction associated with aberrant formation of osteoclasts in WT mice, but the level of bone destruction was much less pronounced and the osteoclast formation was significantly reduced in both the *Il17*$^{-/-}$ mice and *Il23a*$^{-/-}$ mice (Fig. 4 D). These results suggest that the Th17 cells expanded through IL-23 stimulation are involved in the T cell–mediated osteoclastogenesis in vivo. In contrast, the bone destruction was enhanced and a greater number of osteoclasts were formed in *Ifngr1*$^{-/-}$ *Stat6*$^{-/-}$ mice, which are deficient in the response to both IFN-γ and IL-4 (Fig. 4 D), suggesting that IFN-γ and IL-4 may play a protective role against bone destruction by suppressing osteoclastogenesis associated with inflammation.

The above results suggest that IL-23–stimulated proliferation of Th17 cells, a major osteoclastogenic Th subset, plays a pivotal role in inflammatory bone destruction by inducing RANKL through an IL-17 effect on mesenchymal cells. Consistent with this, it has been reported that RANKL is abundantly expressed in the synovial fibroblasts of RA patients (16, 40) and the IL-17 concentration is elevated in the synovial fluid of RA patients (25). To explore the role of IL-23 in the induction of RANKL in RA, we investigated whether IL-23 was detected in the synovium of RA patients. Quantitative RT-PCR analysis revealed the mRNA of the p19 subunit of IL-23 (*IL23A*) in all the samples of the synovium derived from RA patients, and the expression level of *IL23A* positively correlated with that of *RANKL* (Fig. 5 A). A similar correlation was observed between *RANKL* and the p40 subunit shared by IL-12 and IL-23 (*IL12B*), but the expression of the p35 subunit specific for IL-12 (*IL12A*) did not correlate with that of *RANKL*, suggesting that IL-23 is an important determinant of arthritic bone destruction through the induction of RANKL. These results lend further support to the notion that the IL-23–IL-17 axis, rather than the IL-12–IFN-γ axis, is critical for the bone destruction phase of autoimmune arthritis.

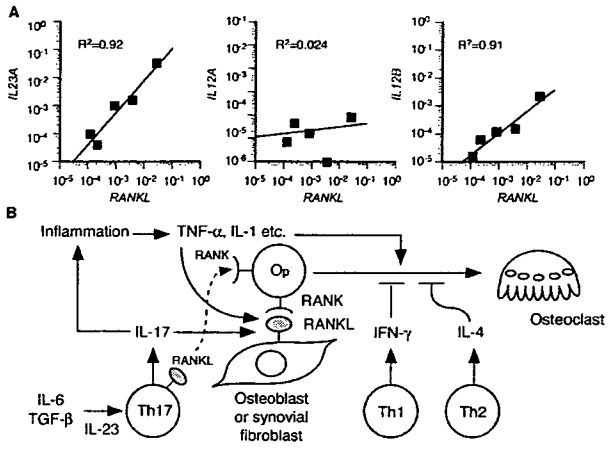

Figure 5. Regulation of RANKL-mediated osteoclastogenesis by the IL-23–IL-17 axis in the RA synovial tissue. (A) Correlation of the mRNA expression level of RANKL with that of *IL23A* (*p19*), *IL12A* (*p35*), or *IL12B* (*p40*) in the synovium of RA patients. The relative expressions of *RANKL*, *IL23A*, *IL12A*, and *IL12B* were all standardized using that of *GAPDH*. (B) Model of Th17-mediated bone destruction in autoimmune arthritis. Th17 cells function as an osteoclastogenic Th cell subset by stimulating local inflammation, inducing RANKL on osteoclastogenesis-supporting cells, and expressing RANKL on themselves, all of which contribute to an acceleration of osteoclastogenesis. It is notable that RANKL on Th17 cells alone is not sufficient for the induction of osteoclast differentiation (a dotted line). See Discussion for the details. Op, osteoclast precursor cell.

DISCUSSION

Coordinated activation of the innate and adaptive immune systems is essential for the efficient eradication of pathogens, but aberrant or prolonged activation under certain pathological conditions, such as autoimmune inflammation, results in tissue damage through the activation of effector cells. In autoimmune arthritis, it has long been a challenging question as to how the abnormality of the immune system induces the skeletal damage, although the infiltration of CD4$^+$ T cells in the RA synovium is a pathogenetic hallmark and is undoubtedly linked to the bone destruction that ensues (3, 13, 14, 20). After RANKL was cloned and the high RANKL expression in the synovium was brought to light (16, 40), the importance of bone-resorbing osteoclasts came into general acceptance (3). Based on recent reports using genetically modified mice, the crucial role of osteoclasts in the inflammatory bone loss has been established (41, 42), but which CD4$^+$ T cells cause the induction of osteoclasts, and by what mechanism, has remained elusive.

As RANKL is expressed in activated T cells, T cells may have the capacity to induce osteoclast differentiation by directly acting on osteoclast precursor cells (13, 26). However, because T cells also secrete a variety of cytokines and express membrane-bound factors other than RANKL, the effects of T cells on osteoclastogenesis should be dependent on the balance of positive and negative factors expressed by the T cells. As summarized in Fig. 5 B, the results in this study show that Th1 and Th2 cells inhibit osteoclastogenesis by acting on the precursor cells, mainly through IFN-γ and IL-4, respectively.

The inhibitory effects of these cytokines were less observed in the co-culture system than in the RANKL–M-CSF system (Figs. 1, B and C, and 2 A). We infer that osteoblasts may provide membrane-bound RANKL and stimulate costimulatory signals for RANKL simultaneously, enabling the strong cell–cell contact between osteoblasts and osteoclast precursor cells and preventing the access of T cells or inhibitory cytokines to osteoclast precursor cells.

Previous observations that IL-12 and IL-18, which drive Th1 differentiation, both inhibit osteoclastogenesis via IFN-γ or GM-CSF (43, 44), and that IL-10, which is released from Th2 cells, also negatively regulates osteoclastogenesis (45) further support the negative role of Th1 and Th2 cells on osteoclastogenesis. In contrast, Th17 cells stimulated by IL-23 promote osteoclastogenesis mostly through production of IL-17 (Fig. 3, A and C). Therefore, the osteoclastogenic ability of Th17 cells does not require cell–cell contact with osteoclast precursor cells, but additional membrane-bound mediators such as RANKL and CD40L may also contribute (46, 47). IL-17 is known to act on the osteoclastogenesis-supporting cells to induce RANKL (25). It should be noted that the effect of IL-17 is not limited to this direct effect on the osteoclastogenesis-supporting cells. IL-17 facilitates local inflammation by recruiting and activating immune cells, which leads to an abundance of inflammatory cytokines such as TNF-α and IL-1 (9, 10). The inflammatory cytokines enhance RANKL expression on osteoclastogenesis-supporting cells and activate osteoclast precursor cells by synergizing with RANKL signaling. A relatively high expression of RANKL on Th17 cells may also participate in the enhanced osteoclastogenesis (Fig. 3 E). Collectively, Th17 cells can be called an osteoclastogenic Th subset not only because Th17 cells have positive effects on osteoclastogenesis in vitro, but also because they tip the balance of the microenvironments in favor of osteoclast differentiation.

It is worth noting that Th17 cells do not induce osteoclastogenesis in the absence of osteoblasts. This strongly suggests that RANKL expressed on Th17 cells alone is not sufficient to induce osteoclastogenesis, although this is partly because even Th17 cells produce a small amount of IFN-γ, which counterbalances the RANKL action. To understand the role of RANKL on T cells in more detail, we need mice of T cell–specific ablation of the *RANKL* gene, which are currently unavailable. But it is conceivable that RANKL expressed on adherent cells such as osteoblasts has more potent effects than that expressed on T cells. This mechanism may also explain why osteoclasts are formed only in the bone microenvironments, but it currently remains to be clarified. We consider the following explanations: (a) T cell expression of membrane-bound RANKL, which is more osteoclastogenic than the soluble form (48), is very low compared with that on osteoblasts; (b) costimulatory signals provided specifically by osteoblasts (12, 27) are missing in T cells; and (c) cell adhesion induces specific signals including those mediated by integrins, which are also important for osteoclastogenesis (49).

In our study, T reg cells had no apparent effect on osteoclastogenesis in vitro (Fig. 1 G). However, their function in the regulation of bone metabolism should be investigated in vivo considering the recent finding that the development of Th17 cells and T reg cells is coordinately regulated (10, 35, 36).

The importance of the IL-23–IL-17 axis in the autoimmune inflammation has been demonstrated in a variety of models of autoimmune diseases such as arthritis and encephalomyelitis (23, 24, 38). In arthritis models, *IL-17*$^{-/-}$ mice were protected from the development of destructive arthritis (24), whereas collagen-induced arthritis is exacerbated in IFN-γ receptor–deficient mice (21, 22). The specific role of IL-23 compared with IL-12 in the development of arthritis has been clearly demonstrated by a genetic study using mice deficient in p19 and p35 (23). Based on these observations, the IL-23–IL-17 axis inducing Th17 cells, rather than the IL-12–IFN-γ axis inducing Th1 cells, is critical for the development of autoimmune arthritis. Our study also provides evidence that the IL-23–IL-17 axis plays a critical role even in a model of bone loss induced by local inflammation that is independent of autoimmunity (Fig. 4 D), suggesting that the IL-23–IL-17 axis is not only essential for the onset phase, but also for the destruction phase of autoimmune arthritis characterized by the T cell–mediated activation of osteoclastogenesis. Thus, Th17 cells, an osteoclastogenic subset, have profound relevance in the bone damage that takes place in autoimmune arthritis. The identification of T cell subsets in the synovium of arthritis is a challenging issue of great importance that should be pursued in a future study. Considering the strong inhibitory effects of Th1 cells on osteoclastogenesis, Th17 cells may be overwhelmingly dominant and the colocalization of Th1 cells is unlikely, at least under the microenvironments in which osteoclastogenesis efficiently occurs. The positive correlation between IL-23 and RANKL expression in the synovium of RA patients further suggests the importance of IL-23 in the regulation of local osteoclastogenesis through IL-17 (Fig. 5 A). Despite the importance of TGF-β and IL-6 in the initiation of Th17 development (10, 35, 36), Th17 cells can be obtained in an IL-23–stimulated culture system without adding exogenous TGF-β/IL-6, suggesting that the endogenous level of TGF-β/IL-6 may suffice for the initiation and that osteoclastogenic activity of Th17 cells is mainly determined by IL-23 under certain pathological conditions.

For the treatment of RA, there are several drugs available, most of which were developed to modulate immune reactions. The antirheumatic drugs are effective in treating pain and inflammation, but patients still fairly frequently have to undergo joint replacement surgery because of the progressive bone damage despite long-term treatment with antirheumatic drugs. Therefore, it is clinically an urgent issue to establish a method to prevent such persistent bone destruction (3). Although rheumatologists are now aware of the great impact that anti-TNF therapy has had on the management of RA (50), it is still not determined whether all patients respond

to the therapy or, indeed, whether bone destruction will be completely prevented by it. Recent progress in understanding the mechanism of bone loss in RA has provided promising new strategies, one of which is an anti-RANKL antibody directly suppressing RANKL-mediated osteoclastogenesis (51). As we have demonstrated a new role of Th17 in the context of bone damage in RA, the significance of the IL-23–IL-17 axis extends beyond the simple initiation or development of the autoimmunity. Because osteoclastogenic Th17 cells link the autoimmune inflammation to bone damage, inhibition of this axis has the potential of a doubly beneficial impact on RA, i.e., in the context of both the immune and skeletal systems, and thus appears to be an ideal therapeutic strategy for ameliorating the bone destruction associated with T cell activation.

MATERIALS AND METHODS

Mice. *Ifngr1*$^{-/-}$ (28), *Stat6*$^{-/-}$ (30), *Il17*$^{-/-}$ (37), and *Il23a*$^{-/-}$ mice (38) were described previously. All the mice were maintained under specific pathogen-free conditions and were backcrossed to C57BL/6 mice. All animal experiments were performed with the approval of the Animal Study Committee of Tokyo Medical and Dental University and conformed to relevant guidelines and laws.

Analysis of bone phenotype and LPS-induced bone destruction. The mice were subjected to histomorphometric and microradiographic examinations as described previously (27). 8-wk-old mice were injected with 25 mg/kg body weight LPS (Sigma-Aldrich) subperiosteally in the calvarial bone. After 5 d, calvarial bones were analyzed as described previously using decalcified paraffin sections (14).

In vitro assays for osteoclast differentiation and function. In vitro osteoclast differentiation was described previously (27, 52). For the RANKL–M-CSF system, we cultured BMCs with 10 ng/ml M-CSF (R&D Systems) for 2 d and used them as BMMs. The cells were cultured with 50 ng/ml RANKL (PeproTech) and 10 ng/ml M-CSF for 3 d, and TRAP$^+$ multinucleated (more than three nuclei) cells were counted. The co-culture of osteoblasts derived from mouse calvarial cells and BMCs was performed in the presence of 10^{-8} M $VitD_3$ (Wako) and 10^{-6} M PGE_2 (Wako) for 7 d. For the assessment of the bone-resorbing function of osteoclasts, we cultured osteoclast precursors on a hydroxy appatite–coated disc (Osteologic; BD Biosciences). After the culture period, the cells were washed away as described in the manufacturer's protocol by 6% NaOCl and 5.2% NaCl.

Th cell differentiation. CD4$^+$ T cells were purified from the spleen using a magnetic sorter and anti-CD4 microbeads (MACS; Miltenyi Biotec). The purity of the CD4$^+$ T cells was >95%. These CD4$^+$ T cells were stimulated with a plate-bound anti-CD3 mAb and anti-CD28 mAb (1 μg/ml each) for 3 d in the presence of (a) 10 ng/ml IL-12 and 10 μg/ml anti–IL-4 mAb for the Th1 cells, (b) 10 ng/ml IL-4 and 10 μg/ml anti–IFN-γ mAb for the Th2 cells, and (c) 10 ng/ml IL-23 along with 10 μg/ml each of anti–IFN-γ and anti–IL-4 mAbs for the Th17 cells. When indicated, the T cells were added to the culture system with 1 μg/ml anti-CD3 mAb for restimulation. All the antibodies were purchased from BD Biosciences except for the anti-RANKL mAb (provided by H. Yagita, Juntendo University School of Medicine, Tokyo, Japan). Recombinant IL-17 and the other cytokines were purchased from Genzyme and R&D Systems, respectively. T reg cells were purified using a MACS CD4$^+$CD25$^+$ Regulatory T Cell Isolation kit.

Analysis of mRNAs expressed in RA synovial tissues. Synovial tissues were obtained at the time of total knee arthroplasty from five patients (age range, 55–70 yr) who fulfilled the American College of Rheumatology criteria and gave informed consent (16). The experiments were performed with the approval of the institutional ethical committee. The tissues were minced and homogenized in Sepasol-RNA (Nacalai Tesque), and total RNA was extracted and purified according to the manufacturer's protocol.

GeneChip analysis and quantitative RT-PCR. Total RNA (15 μg) was used for cDNA synthesis by reverse transcription followed by the synthesis of biotinylated cRNA through in vitro transcription. After cRNA fragmentation, we performed hybridization with a mouse A430 GeneChip (Affymetrix, Inc.) (31). We performed quantitative RT-PCR using a LightCycler (Roche), as described previously (52). The following primers were used: *IL23A*: 5′-CTGCTTGCAAAGGATCCACC-3′ (sense), 5′-TTGAAGCGGAGAAGGAGACG-3′ (antisense); *IL12A*: 5′-AGCCTCCTCCTTGTGGCTA-3′ (sense), 5′-TGTGCTGGTTTTATCTTTTGTG-3′ (antisense); *IL12B*: 5′-TCACAAAGGAGGCGAGGTT-3′ (sense), 5′-ATGACCTCAATGGGCAGACTC-3′ (antisense); and *RANKL*: 5′-AACCAGATGGGATGTCGGTGGCATTA-3′ (sense), 5′-AGCGATGGTGGATGGCTCATGGTTAG-3′ (antisense). The level of mRNA expression was normalized with that of *GAPDH* expression in Fig. 5 A.

Statistical analyses. All data were expressed as the mean ± SEM ($n = 4$, unless otherwise indicated). Mann-Whitney U test was used for statistical analyses (*, $P < 0.05$; **, $P < 0.01$), and comparisons were made between each sample and the control (not treated with T cells/cytokines or WT mice).

Online supplemental material. Fig. S1 shows the effect of recombinant IL-4 on osteoclast precursor cells derived from WT or *Stat6*$^{-/-}$ mice in the RANKL–M-CSF system. Fig. S2 shows the list of genes whose expression was increased by IL-4 in osteoclast precursor cells (GeneChip analysis). Figs. S1 and S2 are available at http://www.jem.org/cgi/content/full/jem.20061775/DC1.

We are grateful to H. Yagita for providing anti-RANKL mAb. We also thank T. Taniguchi, S. Hida, S. Taki, H. Murayama, J. Taka, M. Asagiri, M. Shinohara, T. Nakashima, H.J. Gober, T. Koga, Y. Sato, and I. Takayanagi for fruitful discussion and assistance.

This work was supported in part by Grant-in-Aid for Creative Scientific Research from Japan Society for the Promotion of Science (JSPS), SORST program of JST, grants for Genome Network Project from the Ministry of Education, Culture, Sports, Science, and Technology of Japan (MEXT), grants for the 21st century COE program from MEXT, Grants-in-Aid for Scientific Research from MEXT, Health Sciences Research Grants from the Ministry of Health, Labor and Welfare of Japan, and grants from the Naito Foundation, Suzuken Memorial Foundation, Uehara Memorial Foundation, Kato Memorial Bioscience Foundation, Cell Science Research Foundation, Inamori Foundation, and the Nakatomi Foundation.

The authors have no conflicting financial interests.

Submitted: 18 August 2006
Accepted: 12 October 2006

REFERENCES

1. Walsh, M.C., N. Kim, Y. Kadono, J. Rho, S.Y. Lee, J. Lorenzo, and Y. Choi. 2006. Osteoimmunology: interplay between the immune system and bone metabolism. *Annu. Rev. Immunol.* 24:33–63.
2. Takayanagi, H. 2005. Inflammatory bone destruction and osteoimmunology. *J. Periodontal Res.* 40:287–293.
3. Sato, K., and H. Takayanagi. 2006. Osteoclasts, rheumatoid arthritis, and osteoimmunology. *Curr. Opin. Rheumatol.* 18:419–426.
4. Theill, L.E., W.J. Boyle, and J.M. Penninger. 2002. RANK-L and RANK: T cells, bone loss, and mammalian evolution. *Annu. Rev. Immunol.* 20:795–823.
5. Teitelbaum, S.L., and F.P. Ross. 2003. Genetic regulation of osteoclast development and function. *Nat. Rev. Genet.* 4:638–649.
6. Boyle, W.J., W.S. Simonet, and D.L. Lacey. 2003. Osteoclast differentiation and activation. *Nature.* 423:337–342.
7. Suda, T., N. Takahashi, N. Udagawa, E. Jimi, M.T. Gillespie, and T.J. Martin. 1999. Modulation of osteoclast differentiation and function by the new members of the tumor necrosis factor receptor and ligand families. *Endocr. Rev.* 20:345–357.

8. Mosmann, T.R., H. Cherwinski, M.W. Bond, M.A. Giedlin, and R.L. Coffinan. 1986. Two types of murine helper T cell clone. I. Definition according to profiles of lymphokine activities and secreted proteins. *J. Immunol.* 136:2348–2357.
9. Dong, C. 2006. Diversification of T-helper-cell lineages: finding the family root of IL-17-producing cells. *Nat. Rev. Immunol.* 6:329–333.
10. Weaver, C.T., L.E. Harrington, P.R. Mangan, M. Gavrieli, and K.M. Murphy. 2006. Th17: an effector CD4 T cell lineage with regulatory T cell ties. *Immunity.* 24:677–688.
11. Sakaguchi, S. 2005. Naturally arising Foxp3-expressing $CD25^+CD4^+$ regulatory T cells in immunological tolerance to self and non-self. *Nat. Immunol.* 6:345–352.
12. Takayanagi, H. 2005. Mechanistic insight into osteoclast differentiation in osteoimmunology. *J. Mol. Med.* 83:170–179.
13. Kong, Y.Y., U. Feige, I. Sarosi, B. Bolon, A. Tafuri, S. Morony, C. Capparelli, J. Li, R. Elliott, S. McCabe, et al. 1999. Activated T cells regulate bone loss and joint destruction in adjuvant arthritis through osteoprotegerin ligand. *Nature.* 402:304–309.
14. Takayanagi, H., K. Ogasawara, S. Hida, T. Chiba, S. Murata, K. Sato, A. Takaoka, T. Yokochi, H. Oda, K. Tanaka, et al. 2000. T-cell-mediated regulation of osteoclastogenesis by signalling cross-talk between RANKL and IFN-γ. *Nature.* 408:600–605.
15. Hofbauer, L.C., D.L. Lacey, C.R. Dunstan, T.C. Spelsberg, B.L. Riggs, and S. Khosla. 1999. Interleukin-1β and tumor necrosis factor-α, but not interleukin-6, stimulate osteoprotegerin ligand gene expression in human osteoblastic cells. *Bone.* 25:255–259.
16. Takayanagi, H., H. Iizuka, T. Juji, T. Nakagawa, A. Yamamoto, T. Miyazaki, Y. Koshihara, H. Oda, K. Nakamura, and S. Tanaka. 2000. Involvement of receptor activator of nuclear factor κB ligand/osteoclast differentiation factor in osteoclastogenesis from synoviocytes in rheumatoid arthritis. *Arthritis Rheum.* 43:259–269.
17. Dolhain, R.J., A.N. van der Heiden, N.T. ter Haar, F.C. Breedveld, and A.M. Miltenburg. 1996. Shift toward T lymphocytes with a T helper 1 cytokine-secretion profile in the joints of patients with rheumatoid arthritis. *Arthritis Rheum.* 39:1961–1969.
18. Smolen, J.S., M. Tohidast-Akrad, A. Gal, M. Kunaver, G. Eberl, P. Zenz, A. Falus, and G. Steiner. 1996. The role of T-lymphocytes and cytokines in rheumatoid arthritis. *Scand. J. Rheumatol.* 25:1–4.
19. Husby, G., and R.C. Williams Jr. 1985. Immunohistochemical studies of interleukin-2 and γ-interferon in rheumatoid arthritis. *Arthritis Rheum.* 28:174–181.
20. Kinne, R.W., E. Palombo-Kinne, and F. Emmrich. 1997. T-cells in the pathogenesis of rheumatoid arthritis villains or accomplices? *Biochim. Biophys. Acta.* 1360:109–141.
21. Manoury-Schwartz, B., G. Chiocchia, N. Bessis, O. Abehsira-Amar, F. Batteux, S. Muller, S. Huang, M.C. Boissier, and C. Fournier. 1997. High susceptibility to collagen-induced arthritis in mice lacking IFN-γ receptors. *J. Immunol.* 158:5501–5506.
22. Vermeire, K., H. Heremans, M. Vandeputte, S. Huang, A. Billiau, and P. Matthys. 1997. Accelerated collagen-induced arthritis in IFN-γ receptor-deficient mice. *J. Immunol.* 158:5507–5513.
23. Murphy, C.A., C.L. Langrish, Y. Chen, W. Blumenschein, T. McClanahan, R.A. Kastelein, J.D. Sedgwick, and D.J. Cua. 2003. Divergent pro- and antiinflammatory roles for IL-23 and IL-12 in joint autoimmune inflammation. *J. Exp. Med.* 198:1951–1957.
24. Nakae, S., A. Nambu, K. Sudo, and Y. Iwakura. 2003. Suppression of immune induction of collagen-induced arthritis in IL-17-deficient mice. *J. Immunol.* 171:6173–6177.
25. Kotake, S., N. Udagawa, N. Takahashi, K. Matsuzaki, K. Itoh, S. Ishiyama, S. Saito, K. Inoue, N. Kamatani, M.T. Gillespie, et al. 1999. IL-17 in synovial fluids from patients with rheumatoid arthritis is a potent stimulator of osteoclastogenesis. *J. Clin. Invest.* 103: 1345–1352.
26. Horwood, N.J., V. Kartsogiannis, J.M. Quinn, E. Romas, T.J. Martin, and M.T. Gillespie. 1999. Activated T lymphocytes support osteoclast formation *in vitro*. *Biochem. Biophys. Res. Commun.* 265: 144–150.
27. Koga, T., M. Inui, K. Inoue, S. Kim, A. Suematsu, E. Kobayashi, T. Iwata, H. Ohnishi, T. Matozaki, T. Kodama, et al. 2004. Costimulatory signals mediated by the ITAM motif cooperate with RANKL for bone homeostasis. *Nature.* 428:758–763.
28. Huang, S., W. Hendriks, A. Althage, S. Hemmi, H. Bluethmann, R. Kamijo, J. Vilcek, R.M. Zinkernagel, and M. Aguet. 1993. Immune response in mice that lack the interferon-γ receptor. *Science.* 259:1742–1745.
29. Huang, W., R.J. O'Keefe, and E.M. Schwarz. 2003. Exposure to receptor-activator of NFκB ligand renders pre-osteoclasts resistant to IFN-γ by inducing terminal differentiation. *Arthritis Res. Ther.* 5:R49–R59.
30. Takeda, K., T. Tanaka, W. Shi, M. Matsumoto, M. Minami, S. Kashiwamura, K. Nakanishi, N. Yoshida, T. Kishimoto, and S. Akira. 1996. Essential role of Stat6 in IL-4 signalling. *Nature.* 380:627–630.
31. Takayanagi, H., S. Kim, T. Koga, H. Nishina, M. Isshiki, H. Yoshida, A. Saiura, M. Isobe, T. Yokochi, J. Inoue, et al. 2002. Induction and activation of the transcription factor NFATc1 (NFAT2) integrate RANKL signaling in terminal differentiation of osteoclasts. *Dev. Cell.* 3:889–901.
32. Asagiri, M., K. Sato, T. Usami, S. Ochi, H. Nishina, H. Yoshida, I. Morita, E.F. Wagner, T.W. Mak, E. Serfling, and H. Takayanagi. 2005. Autoamplification of NFATc1 expression determines its essential role in bone homeostasis. *J. Exp. Med.* 202:1261–1269.
33. Harrington, L.E., R.D. Hatton, P.R. Mangan, H. Turner, T.L. Murphy, K.M. Murphy, and C.T. Weaver. 2005. Interleukin 17-producing $CD4^+$ effector T cells develop via a lineage distinct from the T helper type 1 and 2 lineages. *Nat. Immunol.* 6:1123–1132.
34. Park, H., Z. Li, X.O. Yang, S.H. Chang, R. Nurieva, Y.H. Wang, Y. Wang, L. Hood, Z. Zhu, Q. Tian, and C. Dong. 2005. A distinct lineage of CD4 T cells regulates tissue inflammation by producing interleukin 17. *Nat. Immunol.* 6:1133–1141.
35. Mangan, P.R., L.E. Harrington, D.B. O'Quinn, W.S. Helms, D.C. Bullard, C.O. Elson, R.D. Hatton, S.M. Wahl, T.R. Schoeb, and C.T. Weaver. 2006. Transforming growth factor-β induces development of the T_H17 lineage. *Nature.* 441:231–234.
36. Bettelli, E., Y. Carrier, W. Gao, T. Korn, T.B. Strom, M. Oukka, H.L. Weiner, and V.K. Kuchroo. 2006. Reciprocal developmental pathways for the generation of pathogenic effector T_H17 and regulatory T cells. *Nature.* 441:235–238.
37. Nakae, S., Y. Komiyama, A. Nambu, K. Sudo, M. Iwase, I. Homma, K. Sekikawa, M. Asano, and Y. Iwakura. 2002. Antigen-specific T cell sensitization is impaired in IL-17-deficient mice, causing suppression of allergic cellular and humoral responses. *Immunity.* 17:375–387.
38. Cua, D.J., J. Sherlock, Y. Chen, C.A. Murphy, B. Joyce, B. Seymour, L. Lucian, W. To, S. Kwan, T. Churakova, et al. 2003. Interleukin-23 rather than interleukin-12 is the critical cytokine for autoimmune inflammation of the brain. *Nature.* 421:744–748.
39. Ukai, T., Y. Hara, and I. Kato. 1996. Effects of T cell adoptive transfer into nude mice on alveolar bone resorption induced by endotoxin. *J. Periodontal Res.* 31:414–422.
40. Gravallese, E.M., C. Manning, A. Tsay, A. Naito, C. Pan, E. Amento, and S.R. Goldring. 2000. Synovial tissue in rheumatoid arthritis is a source of osteoclast differentiation factor. *Arthritis Rheum.* 43: 250–258.
41. Pettit, A.R., H. Ji, D. von Stechow, R. Muller, S.R. Goldring, Y. Choi, C. Benoist, and E.M. Gravallese. 2001. TRANCE/RANKL knockout mice are protected from bone erosion in a serum transfer model of arthritis. *Am. J. Pathol.* 159:1689–1699.
42. Redlich, K., S. Hayer, R. Ricci, J.P. David, M. Tohidast-Akrad, G. Kollias, G. Steiner, J.S. Smolen, E.F. Wagner, and G. Schett. 2002. Osteoclasts are essential for TNF-α-mediated joint destruction. *J. Clin. Invest.* 110:1419–1427.
43. Horwood, N.J., J. Elliott, T.J. Martin, and M.T. Gillespie. 2001. IL-12 alone and in synergy with IL-18 inhibits osteoclast formation *in vitro*. *J. Immunol.* 166:4915–4921.
44. Udagawa, N., N.J. Horwood, J. Elliott, A. Mackay, J. Owens, H. Okamura, M. Kurimoto, T.J. Chambers, T.J. Martin, and M.T. Gillespie. 1997. Interleukin-18 (interferon-γ–inducing factor) is produced by osteoblasts and acts via granulocyte/macrophage colony-stimulating factor and not via interferon-γ to inhibit osteoclast formation. *J. Exp. Med.* 185:1005–1012.

45. Hong, M.H., H. Williams, C.H. Jin, and J.W. Pike. 2000. The inhibitory effect of interleukin-10 on mouse osteoclast formation involves novel tyrosine-phosphorylated proteins. *J. Bone Miner. Res.* 15:911–918.
46. Kadono, Y., F. Okada, C. Perchonock, H.D. Jang, S.Y. Lee, N. Kim, and Y. Choi. 2005. Strength of TRAF6 signalling determines osteoclastogenesis. *EMBO Rep.* 6:171–176.
47. Gohda, J., T. Akiyama, T. Koga, H. Takayanagi, S. Tanaka, and J. Inoue. 2005. RANK-mediated amplification of TRAF6 signaling leads to NFATc1 induction during osteoclastogenesis. *EMBO J.* 24: 790–799.
48. Hikita, A., Y. Kadono, H. Chikuda, A. Fukuda, H. Wakeyama, H. Yasuda, K. Nakamura, H. Oda, T. Miyazaki, and S. Tanaka. 2005. Identification of an alternatively spliced variant of Ca^{2+}-promoted Ras inactivator as a possible regulator of RANKL shedding. *J. Biol. Chem.* 280:41700–41706.
49. Ross, F.P., and S.L. Teitelbaum. 2005. $\alpha v\beta 3$ and macrophage colony-stimulating factor: partners in osteoclast biology. *Immunol. Rev.* 208: 88–105.
50. Palladino, M.A., F.R. Bahjat, E.A. Theodorakis, and L.L. Moldawer. 2003. Anti-TNF-α therapies: the next generation. *Nat. Rev. Drug Discov.* 2:736–746.
51. McClung, M.R., E.M. Lewiecki, S.B. Cohen, M.A. Bolognese, G.C. Woodson, A.H. Moffett, M. Peacock, P.D. Miller, S.N. Lederman, C.H. Chesnut, et al. 2006. Denosumab in postmenopausal women with low bone mineral density. *N. Engl. J. Med.* 354:821–831.
52. Kim, Y., K. Sato, M. Asagiri, I. Morita, K. Soma, and H. Takayanagi. 2005. Contribution of nuclear factor of activated T cells c1 to the transcriptional control of immunoreceptor osteoclast-associated receptor but not triggering receptor expressed by myeloid cells-2 during osteoclastogenesis. *J. Biol. Chem.* 280:32905–32913.

Cell

Force Sensing by Mechanical Extension of the Src Family Kinase Substrate p130Cas

Yasuhiro Sawada,[1,*] Masako Tamada,[1] Benjamin J. Dubin-Thaler,[1] Oksana Cherniavskaya,[1] Ryuichi Sakai,[2] Sakae Tanaka,[3] and Michael P. Sheetz[1]
[1] Department of Biological Sciences, Columbia University, Sherman Fairchild Center Room 715, MC-2416, 1212 Amsterdam Avenue, New York, NY 10027, USA
[2] Growth Factor Division, National Cancer Center Research Institute, 5-1-1 Tsukiji, Chuo-ku, Tokyo 104-0045, Japan
[3] Department of Orthopaedic Surgery, Graduate School of Medicine, The University of Tokyo, 7-3-1 Hongo, Bunkyo-ku, Tokyo 113-0033, Japan
*Contact: ys454-ind@umin.ac.jp
DOI 10.1016/j.cell.2006.09.044

SUMMARY

How physical force is sensed by cells and transduced into cellular signaling pathways is poorly understood. Previously, we showed that tyrosine phosphorylation of p130Cas (Cas) in a cytoskeletal complex is involved in force-dependent activation of the small GTPase Rap1. Here, we mechanically extended bacterially expressed Cas substrate domain protein (CasSD) in vitro and found a remarkable enhancement of phosphorylation by Src family kinases with no apparent change in kinase activity. Using an antibody that recognized extended CasSD in vitro, we observed Cas extension in intact cells in the peripheral regions of spreading cells, where higher traction forces are expected and where phosphorylated Cas was detected, suggesting that the in vitro extension and phosphorylation of CasSD are relevant to physiological force transduction. Thus, we propose that Cas acts as a primary force sensor, transducing force into mechanical extension and thereby priming phosphorylation and activation of downstream signaling.

INTRODUCTION

Cellular responses to mechanical force underlie many critical functions, from normal morphogenesis to carcinogenesis, cardiac hypertrophy, wound healing, and bone homeostasis. Recent studies indicate that various signaling pathways are involved in force transduction, including MAP kinases, small GTPases, and tyrosine kinases/phosphatases (Geiger and Bershadsky, 2002; Giannone and Sheetz, 2006; Katsumi et al., 2002; Sawada et al., 2001). A variety of primary force-sensing mechanisms could be postulated, including mechanical extension of cytoplasmic proteins, activation of ion channels, and formation of force-stabilized receptor-ligand bonds (catch bonds) (Vogel and Sheetz, 2006), which would then activate downstream signaling pathways. At a biochemical level, tyrosine phosphorylation levels appear to be linked to mechanically induced changes controlling many other cellular functions (Giannone and Sheetz, 2006). One protein involved in mechanically induced phosphorylation-dependent signaling is the Src family kinase substrate Cas (Crk-associated substrate), which is involved in various cellular events such as migration, survival, transformation, and invasion (Defilippi et al., 2006). Stretch-dependent tyrosine phosphorylation of Cas by Src family kinases (SFKs) occurs in detergent-insoluble cytoskeletal complexes and is involved in force-dependent activation of the small GTPase Rap1 (Tamada et al., 2004). Rap1 is activated by distinct types of guanine nucleotide exchange factors coupled with various receptors or second messengers and plays an important role in a number of signaling pathways, including integrin signaling (Hattori and Minato, 2003).

The Cas substrate domain, which is located in the center of Cas, is flanked by the amino-terminal SH3 and the carboxy-terminal Src-binding domains. These amino- and carboxy-terminal domains are involved in Cas localization at focal adhesions, while the substrate domain itself is not (Nakamoto et al., 1997), suggesting that these flanking domains anchor Cas molecules to the cytoskeletal complex and that the substrate domain could be extended upon cytoskeleton stretching. Furthermore, the Cas substrate domain has 15 repeats of a tyrosine-containing motif (YxxP) (Mayer et al., 1995), and multiple sequence repeats are found in molecules with mechanical functions such as titin (Rief et al., 1997).

Cell stretching could increase tyrosine phosphorylation by (1) directly activating the kinase, (2) inactivating the phosphatase, (3) mechanically bringing the kinase to the substrate, or (4) enhancing the susceptibility of the substrate to phosphorylation. To test between these possibilities, we have analyzed the mechanisms of stretch-dependent

enhancement of Cas phosphorylation. In intact cells, Cas phosphorylation by c-Src is significantly increased by cell stretching with no detectable change in c-Src kinase activity. Cas phosphorylation mediates physiological force transduction through stretch-dependent activation of Rap1 in intact cells. With *in vitro protein extension* (IPE) experiments, we find that phosphorylation of CasSD by specific kinases is increased upon extension. Further, an antibody that recognizes extended CasSD in vitro preferentially recognizes Cas molecules at the periphery of late spreading cells where higher traction forces are predicted and Cas is phosphorylated, indicating that the in vitro extension and phosphorylation of CasSD is relevant to force transduction through Cas phosphorylation in intact cells. Thus, we suggest that Cas serves as a direct mechanosensor where force induces a mechanical extension of the substrate domain that primes it for phosphorylation. We propose that such "substrate priming" is a general mechanism for force transduction.

RESULTS

Cell Stretching Enhances SFK-Dependent Phosphorylation of Cas without a Detectable Increase in Src Kinase Activity

We first examined whether the phosphorylation of Cas increased upon intact cell stretching, using the cell stretching system that we developed (Sawada et al., 2001). Cells were cultured on a stretchable substrate (collagen-coated silicone), and the substrate was stretched uniformly and biaxially (10% in each dimension) and held stretched. To analyze the primary responses to cell stretching, samples were prepared from the cells lysed shortly (1 min) after stretching. Immunoblotting using an anti-phospho-Cas antibody (pCas-165) that specifically recognizes multiple phosphorylated YxxP motifs in the substrate domain (Fonseca et al., 2004) revealed a stretch-dependent increase in tyrosine phosphorylation of Cas in HEK293 cells (Figure 1A). When the selective SFK inhibitor CGP77675 (Missbach et al., 1999) (Novartis Pharma AG, Switzerland) was added prior to stretching, stretch-dependent tyrosine phosphorylation of Cas was inhibited (Figure 1A). Furthermore, stretch-dependent phosphorylation of Cas was greatly attenuated in SYF cells that lacked the major SFKs, c-Src, c-Yes, and Fyn (Klinghoffer et al., 1999), and was restored in SYF cells stably expressing c-Src (Figure 1B), c-Yes, or Fyn (data not shown). Thus, stretching intact cells increased tyrosine phosphorylation of Cas by SFKs.

To determine if stretch-dependent increases in Cas phosphorylation correlated with SFK activation, the levels of c-Src phosphorylation at either activating or inhibiting tyrosine residue (Y416 and Y527, respectively) were examined in SYF cells stably expressing c-Src, either stretched or left unstretched. We observed no changes in phosphorylation levels of those tyrosines (pY416 and pY527) (Figure 1B, lanes 3 and 4). Since the levels of pY416 and pY527 indicate Src kinase inhibition and activation, respectively (Thomas and Brugge, 1997), cell stretching did not appear to affect c-Src activity, while Cas phosphorylation significantly increased. This was further confirmed by an in vitro kinase assay of immunoprecipitated c-Src (Figure 1C). Thus, stretching intact cells increased tyrosine phosphorylation of Cas by c-Src without detectable enhancement of c-Src kinase activity.

Tyrosine Phosphorylation of Cas Is Involved in Stretch-Dependent Rap1 Activation

To explore the role of Cas in physiological force transduction pathways, we analyzed the involvement of Cas in the stretch-dependent activation of Rap1 in cells (Sawada et al., 2001). When the level of Cas protein and phosphorylated Cas was selectively decreased by small interfering RNA (siRNA) in HEK293 cells (Figure 2A, upper panel), Rap1 activity in cells, either stretched or unstretched, was significantly attenuated (Figure 2A, lower panel). Thus, Cas plays a significant role in the stretch-dependent activation of Rap1 in intact cells. However, there is likely more than one pathway for Rap1 activation, considering the fold decrease of Rap1 activity (~50%) in Cas knockdown cells (Figure 2A) as well as the stretch-dependent Rap1 activation observed in Cas-deficient fibroblasts (data not shown).

To further examine the role of phosphorylation of Cas in stretch-dependent Rap1 activation, we overexpressed Cas together with Rap1 in HEK293 cells. Upon coexpression of monomeric red fluorescent protein (RFP)-tagged wild-type Cas (RFP-Cas) with green fluorescent protein (GFP)-tagged Rap1 (GFP-Rap1), stretch-dependent activity of GFP-Rap1 was enhanced over the cells coexpressing RFP alone or RFP-Cas15YF that had all 15 YxxP motifs in the substrate domain mutated to FxxP (Figure 2B). The fold increase of Rap1 activity by cell stretching appeared to be smaller in the case of RFP-Cas-expressing cells, probably due to the less efficient incorporation of "overexpressed" Cas into physiological signaling complexes. However, we conclude that tyrosine phosphorylation of Cas is responsible for a significant fraction of the stretch-dependent Rap1 activation.

In Vitro Extension of CasSD

Because kinase activation did not appear to be the primary mechanism regulating Cas phosphorylation in response to cell stretching (Figures 1B and 1C), we tested whether the mechanical extension of the Cas substrate domain modulated its susceptibility to phosphorylation by SFKs. To eliminate the involvement of any extraneous molecules, we performed biochemical analysis, using an IPE system. In that system, bacterially expressed Cas substrate domain protein, CasSD (Cas115–420), was biotinylated on both amino and carboxy termini (designated NC-biotinylated CasSD, Figure 3A, top) and was bound to avidin covalently immobilized on a latex substrate (Figure 3A). After stretching of the latex membrane (Figure 3A), biochemical analyses were performed.

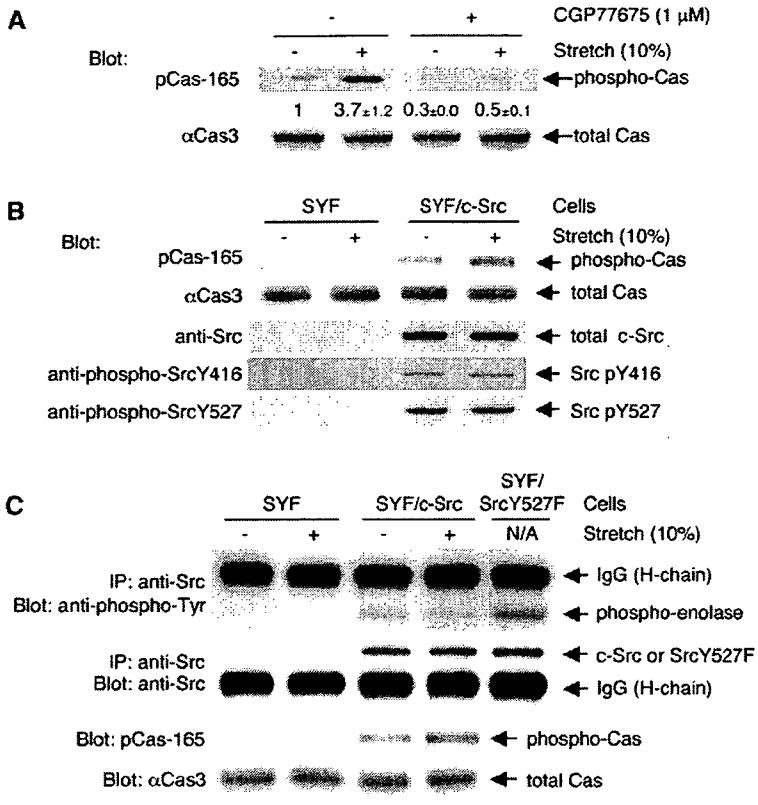

Figure 1. SFK- and Stretch-Dependent Tyrosine Phosphorylation of Cas In Vivo

(A) Stretch-dependent tyrosine phosphorylation of Cas in intact cells. HEK293 (2×10^5) cells on the collagen (type I)-coated stretchable silicone dish were treated with either CGP77675 (1 μM) or its vehicle (0.01% DMSO) and were either stretched (biaxially, 10% in each dimension) or left unstretched. One minute after stretching or without stretching, the cells were solubilized with 1× SDS sample buffer containing 20 mM DTT and analyzed for Cas phosphorylation by anti-phospho-Cas (pCas-165) and anti-Cas (αCas3) immunoblotting. Quantification of phosphorylation (phospho-Cas/total Cas) was scaled with unstretched control set at 1 and noted below the pCas-165 blot with SD (n = 4).

(B) Cell stretching increases Src-dependent phosphorylation of Cas without apparent change in phosphorylation levels of activating and inhibiting tyrosines of c-Src. SYF cells (triple knockout cells of c-src, c-yes, and fyn) or SYF cells stably expressing c-Src (4×10^5) were either stretched or left unstretched. One minute after stretching or without stretching, cells were solubilized with SDS sample buffer, and equivalent portions of each sample were subjected to SDS-PAGE followed by pCas-165, αCas3, anti-Src, anti-phospho-Src Y416, and anti-phospho-Src Y527 immunoblotting.

(C) Cell stretching increases Src-dependent phosphorylation of Cas without apparent change in Src kinase activity. SYF cells or SYF cells stably expressing c-Src (4×10^5) were either stretched or left unstretched. One minute after stretching or without stretching, cells were lysed and subjected to immunoprecipitation followed by an in vitro kinase assay using acid-treated enolase as a substrate. Src kinase activity was analyzed by measuring the phosphorylation of enolase with anti-phospho-tyrosine immunoblotting (top panel). Immunoprecipitated Src, i.e., Src protein in the kinase reaction, was quantified by anti-Src immunoblotting (second panel). Equivalent small portions of each lysate were mixed with SDS sample buffer and subjected directly to SDS-PAGE followed by pCas-165 and αCas3 immunoblotting to analyze for Cas phosphorylation (third and fourth panels). Kinase reactions for the lane 3 and 4 samples appeared not to be saturated because the sample prepared from SYF/SrcY527F cells (SYF cells expressing SrcY527F, the highly active mutant form of c-Src) cultured on a plastic plate following the same protocol gave more phosphorylation of enolase (lane 5). The intense bands above enolase (top panel) and below Src (second panel) represent IgG (heavy chain) from the anti-Src antibody.

To determine if stretching of the latex membrane actually extended NC-biotinylated CasSD, we developed the yellow fluorescent protein (YFP) amino-terminal swapping assay based on the interaction between the amino- and carboxy-terminal regions of YFP. In this assay, CasSD extension was detected by the separation of YFP components attached to the ends of CasSD, causing the binding of an exogenous YFP component. When the two halves of a split YFP, YFP-N and YFP-C, were fused to the amino- and carboxy-terminal ends of NC-biotinylated CasSD, respectively (NY/CY-NC-biotinylated CasSD, Figure 3B), we observed yellow fluorescence in both NY/CY-NC-biotinylated CasSD-expressing bacteria and the purified protein, as expected (Hu et al., 2002). When we added purified His_6-YFP-N to bind to YFP-C in NY/CY-NC biotinylated CasSD (Figure 3B, top), His_6-YFP-N binding was not observed without latex membrane stretching (Figure 3C, lane 1). However, we observed His_6-YFP-N binding upon stretching (Figure 3C, lane 2). Furthermore, His_6-YFP-N did not bind to NY/CY-C-biotinylated CasSD (the unextendable mono-biotinylated control, Figure 3B, bottom) or NC-biotinylated CasSD (extendable, but with no YFP component, Figure 3A, top) even following stretching (Figure 3C, lanes 3–6). Using His_6-YFP-N together with YFP-C fused to glutathione *S*-transferase (GST) in a GST pull-down experiment, we found that YFP-N bound to YFP-C under the same buffer conditions used in the YFP amino-terminal swapping assay (data not shown). Thus, stretching of the latex membrane separated the YFP halves in NY/CY-NC-biotinylated CasSD and allowed His_6-YFP-N to bind, indicating the extension of CasSD (Figure 3B, top).

Extension-Dependent Phosphorylation of CasSD by Recombinant Tyrosine Kinases In Vitro

Since CasSD could be extended by the IPE system, we examined the effect of extension on tyrosine phosphorylation of CasSD by recombinant active c-Src. While the level of phosphorylation was low without stretching (Figure 4A, lane 1), CasSD phosphorylation increased in proportion

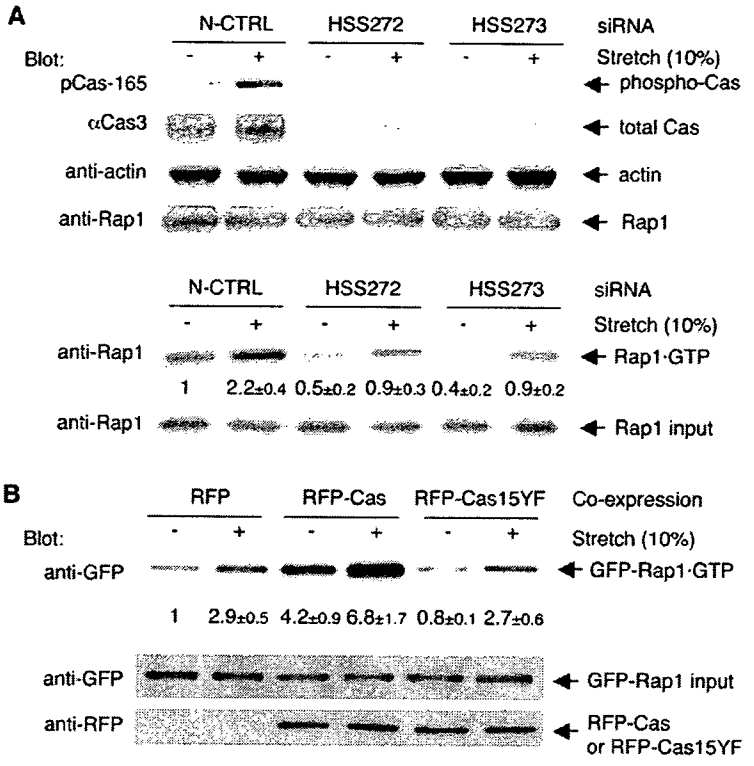

Figure 2. Significant Role of Cas Phosphorylation in Physiological Force Transduction

(A) Cas is involved in stretch-dependent Rap1 activation in intact cells. RNAi experiments were performed as described in the Experimental Procedures. siRNAs used were Stealth RNAi Negative Control Med GC (N-CTRL: lanes 1 and 2), BCAR1-HSS114272 (HSS272: lanes 3 and 4), and BCAR1-HSS114273 (HSS273: lanes 5 and 6) (Invitrogen). Twenty-four hours after transfection, HEK293 cells were either stretched or left unstretched. To determine the level of Cas expression and phosphorylation, cells were solubilized with SDS sample buffer 1 min after stretching or without stretching, and equivalent portions of each sample were subjected to SDS-PAGE followed by anti-phospho-Cas (pCas-165), anti-Cas (αCas3), anti-Rap1, and anti-actin immunoblotting (upper panel). To measure stretch-dependent Rap1 activity, cells were solubilized with lysis buffer for GST pull-down assay (see Experimental Procedures) 5 min after stretching or without stretching. Rap1 was quantified by anti-Rap1 immunoblotting. Rap1 activity (Rap1•GTP/Rap1 input) was scaled with the unstretched control set at 1 and noted below the Rap1•GTP blot with SD (n = 4) (lower panel). The data shown in Figure 2A (upper and lower panels) were obtained with siRNA transfection performed at the same time.

(B) Significant role of tyrosine phosphorylation of Cas in stretch-dependent Rap1 activation. RFP, RFP-Cas, or RFP-Cas15YF was cotransfected with GFP-Rap1 into HEK293 cells (1×10^5/dish). Twenty-four hours after transfection, cells were either stretched or left unstretched. Five minutes after stretching or without stretching, cells were solubilized and subjected to the GST pull-down assay. GFP-Rap1 was quantified by anti-GFP immunoblotting. GFP-Rap1 activity (GFP-Rap1•GTP/GFP-Rap1 input) was scaled with the unstretched RFP-transfected cells set at 1 and noted below the GFP-Rap1•GTP blot with SD (n = 4).

to the magnitude of latex membrane stretching (25%, 50%, 75%, 100%, and 150%) (Figure 4A, lanes 2–6). An unextendable mono-biotinylated CasSD (C-biotinylated CasSD, see Figure 3A, top) was poorly tyrosine phosphorylated either with or without stretching (Figure 4A, lanes 7 and 8). To test if c-Src kinase activity was modulated in the IPE experiments, we added acid-treated enolase to the kinase mixture at the time of kinase reaction and measured its phosphorylation. In the same reaction that gave an extension-dependent increase in CasSD phosphorylation, neither the level of enolase phosphorylation nor the phosphorylation levels of Y416 and Y527 of c-Src kinase were affected by stretching (data not shown). These results indicated that extension-dependent tyrosine phosphorylation of CasSD resulted from CasSD extension and not from an increase in the kinase activity of recombinant c-Src.

We also asked whether or not other kinases phosphorylated CasSD in an extension-dependent manner in IPE experiments. Neither the non-SFK tyrosine kinase Csk (C-terminal Src kinase) nor ZAP-70 phosphorylated NC-biotinylated CasSD, even after stretching (Figure 4B). However, in the same kinase reaction protocol, both Csk and ZAP-70 were able to phosphorylate their known substrates, acid-treated enolase (Bougeret et al., 1993) and the cytoplasmic fragment of human erythrocyte band 3 (cdb3) (Isakov et al., 1996), respectively (data not shown). On the other hand, a known Cas kinase, Abl (Mayer et al., 1995) and another SFK, FynT, phosphorylated CasSD in an extension-dependent manner (Figure 4B). Thus, extension-dependent phosphorylation of CasSD in vitro is caused in a kinase-specific manner, and not by a nonspecific effect of the IPE system.

Although neither the force needed for CasSD extension nor its effect on individual YxxP motifs in CasSD is known, the IPE experiments revealed that different extents of extension induced the phosphorylation of different regions. When we used two different anti-phospho-Cas antibodies (pCas-165 and pCas-410) that had different, though not strictly specific, binding preferences for YxxPs in the Cas substrate domain (Shin et al., 2004) to measure the in vitro CasSD phosphorylation, pCas-410 immunoblotting gave significantly greater fold increase than pCas-165 blots by 40% latex membrane stretching (Figure 4C, left panel). However, pCas-165 and pCas-410 blots showed a similar fold increase by 100% stretching (Figure 4C, right panel). These results suggest that the pCas-410 sites are more efficiently exposed and phosphorylated than pCas-165 sites by smaller extent of CasSD extension.

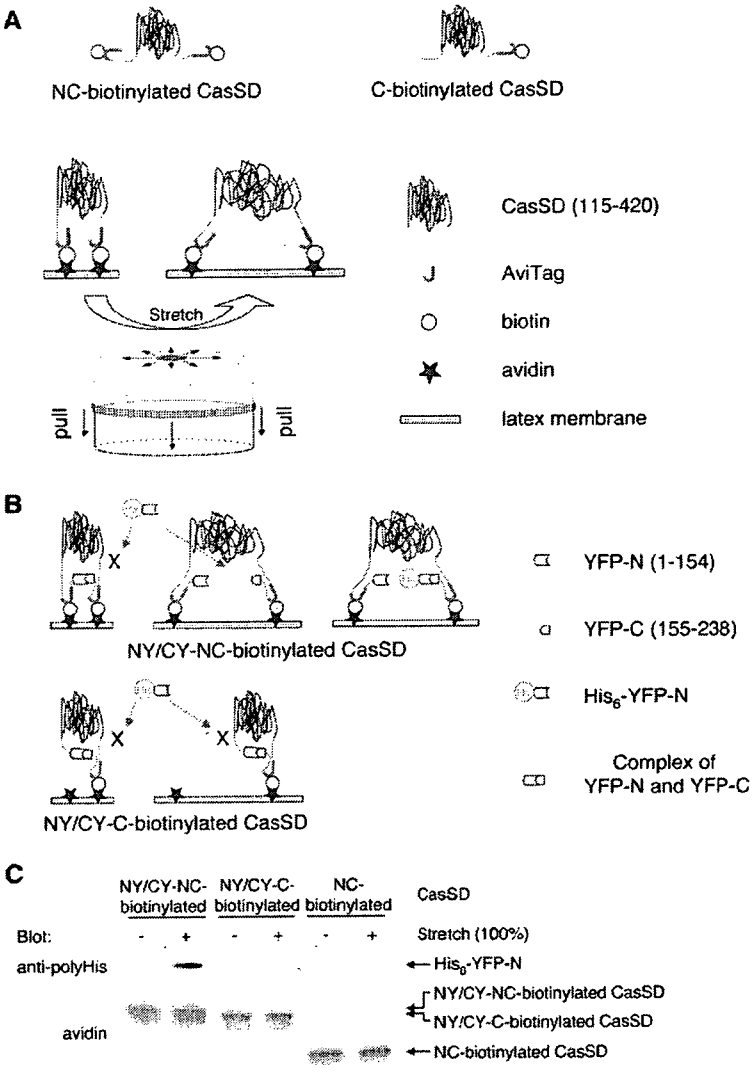

Figure 3. IPE System

(A) Scheme of NC-biotinylated CasSD, C-biotinylated CasSD, and the process of mechanical extension of CasSD in the IPE system.

(B) Schematic description of YFP amino-terminal swapping.

(C) His_6-YFP-N binds to extended NY/CY-NC-biotinylated CasSD, but not to NY/CY-C-biotinylated CasSD or NC-biotinylated CasSD. Biotinylated CasSD proteins, either extended or unextended on latex membrane, were incubated with His_6-YFP-N in the buffer containing 1% Triton X-100 and 1% BSA. After washing, bound complex was solubilized and subjected to SDS-PAGE followed by anti-polyHistidine immunoblotting or avidin affinity blotting.

αCas1, an Antibody that Recognizes Extended CasSD

In order to test if Cas was extended in regions of cell traction forces, we utilized an antibody, αCas1, which was raised against a peptide sequence in the Cas substrate domain (Sakai et al., 1994) (Figure S1A). We found that αCas1 recognized the extended NC-biotinylated CasSD and not the unextended control, C-biotinylated CasSD in the IPE system (Figure 5A). Further, αCas1 bound to SDS-denatured CasSD regardless of its phosphorylation state (Figure S1B), as well as full-length Cas in the SDS-denatured cell lysates (Figure S1C). Thus, αCas1 binding appeared to require the exposure of its epitope in the Cas substrate domain by either extension or denaturation.

Extension of Cas in Triton Cytoskeletons

Using αCas1, we examined whether Cas was extended by stretching Triton cytoskeletons where tyrosine phosphorylation of Cas was observed (Tamada et al., 2004). When we stretched Triton cytoskeletons from Cas-deficient fibroblasts expressing RFP-Cas, we observed a significant increase in αCas1 binding (Figure 5B, lower panel, lanes 1 and 2). Triton cytoskeletons from Cas-deficient fibroblasts expressing RFP alone did not bind αCas1 (Figure 5B, lower panel, lanes 3 and 4). Further, another anti-Cas antibody, αCas3, the epitope of which did not involve the substrate domain (Figure S1A) (Sakai et al., 1994), did not change its binding to Cas in Triton cytoskeletons upon stretching (Figure 5B, lower panel, lanes 5 and 6). These results indicate that the extension of the Cas substrate domain is enhanced by cytoskeleton stretching.

Cas Is Extended at the Sites of High Traction Forces Where Cas Is Phosphorylated In Vivo

Cas extension was difficult to observe in intact cells, since the cell stretching system could not fit onto a total internal